Electrostatic Sensors – Their Principles and Applications

Authors: Yong Yan [a] (Corresponding author)

Yonghui Hu [b]

Lijuan Wang [a]

Xiangchen Qian [b]

Wenbiao Zhang [b]

Kamel Reda [a]

Jiali Wu [b]

Ge Zheng [b]

Addresses: [a] School of Engineering and Digital Arts

University of Kent

Canterbury

Kent CT2 7NT

UK

[b] School of Control and Computer Engineering

North China Electric Power University

Beijing 102206

P. R. China

Email: Y.Yan@kent.ac.uk

ABSTRACT

Over the past three decades electrostatic sensors have been proposed, developed and utilised for the continuous monitoring and measurement of a range of industrial processes, mechanical systems and clinical environments. Electrostatic sensors enjoy simplicity in structure, cost-effectiveness and suitability for a wide range of installation conditions. They either provide unique solutions to some measurement challenges or offer more cost-effective options to the more established sensors such as those based on acoustic, capacitive, optical and electromagnetic principles. The established or potential applications of electrostatic sensors appear wide ranging, but the underlining sensing principle and resultant system characteristics are very similar. This paper presents a comprehensive review of the electrostatic sensors and sensing systems that have been developed for the measurement and monitoring of a range of process variables and conditions. These include the flow measurement of pneumatically conveyed solids, measurement of particulate emissions, monitoring of fluidised beds, on-line particle sizing, burner flame monitoring, speed and radial vibration measurement of mechanical systems, and condition monitoring of power transmission belts, mechanical wear, and human activities. The fundamental sensing principles together with the advantages and limitations of electrostatic sensors for a given area of applications are also introduced. The technology readiness level for each area of applications is identified and commented. Trends and future development of electrostatic sensors, their signal conditioning electronics, signal processing methods as well as possible new applications are also discussed.

Keywords — Electrostatic sensor; triboelectric sensing; electrostatic induction; measurement; condition monitoring

I. INTRODUCTION

Electrostatic phenomena are ubiquitous. When you walk over a plastic floor and then touch a metallic doorknob, you experience a tiny electric shock. Sometimes when you take off your woolen jumper, you may have also experienced a tiny electric spark. Children often rub a balloon on their clothes to make it stick. We can conclude from such common phenomena that static electricity, or electric charge, originates from friction between two different objects. In fact, any close physical contact between two objects though

rubbing will generate static electricity. Such phenomena are widely seen in many industrial processes such as bulk solid handling where significant electrostatic charges are present or even hazardous. Sometimes a close contact between two different objects and then separation without physical friction can also make both electrostatically charged. So, what is the physical mechanism behind this phenomenon? All material comprises of atoms, each of which has a positive nucleus with a number of electrons surrounding it. When two different materials are brought together in close physical contact such as rubbing, one of the material may attract electrons more than the other, so some electrons will be pulled from one material to the other. When the materials are separated, one of them has gained some more electrons (negatively charged) whilst the other has lost some (positively charged), depending on the work function of each material. Such a phenomenon is often known as ***triboelectricity*** or ***triboelectric effect***, where the prefix 'tribo' means friction.

Since triboelectric phenomenon exists widely in our daily lives or industrial activities, electrostatic sensors can be used to detect or sense a diverse range of human activities, mechanical systems or industrial processes. In comparison with more established sensing techniques such as those based on acoustic, resistive, capacitive, piezoelectric, optical and electromagnetic principles, electrostatic sensors are relatively uncommon and less understood. However, electrostatic sensors have clear advantages over other sensors, including cost-effectiveness, high sensitivity, simplicity in system structure and installation, and suitability for a wide range of industrial environments. This monography attempts to pull together the latest developments of electrostatic sensors and their applications in a range of different systems and processes. This monography will introduce the fundamental sensing principles and relevant signal conditioning electronics before introducing the fundamental design and basic characteristics of electrostatic sensors for a wide range of applications. Trends and future developments of electrostatic sensors together with future developments are also discussed. Several different terms are used in the literature to describe electrostatic sensors. In this review we will attempt to review the appropriateness of the terms, but do not intend to unify them.

II. SENSING PRINCIPLES

A. Physical Principle and Terminology

The electrostatic charge is expected on a material whenever it comes into contact with another material or a solid or liquid surface. For instance, a bulk solid material becomes electrostatically charged when it is handled during an industrial process through mixing, sieving, pouring, pulverisation, pneumatic transportation and micronising. The level of charge on the bulk solids is usually unpredictable, but it can be detected with a screened and insulated electrode and an electronic signal conditioning circuit. A signal is derived from the electronic circuit due to the the fluctuations in the electric field resulting from the passage of the charged particles. If the electrode is embedded in an insulator or there is no direct contact between the electrode and the particles, the sensing process is achieved through ***electrostatic induction***. On the contrary, if the electrode is exposed to the fluid flow, ***charge transfer*** due to physical contact between the electrode and the particles will occur. In cases where an exposed electrode is used, both electrostatic induction and charge transfer will take place, though the former is often the dominant interaction. If the insulated electrode is connected to a signal conditioning circuit with an input resistance R_i, the latter will measure the flow of electrons and produce a measurable output. Fig. 1 shows the sensing principle of an exposed electrode to detect a moving non-conducting object in the air through electrostatic induction.

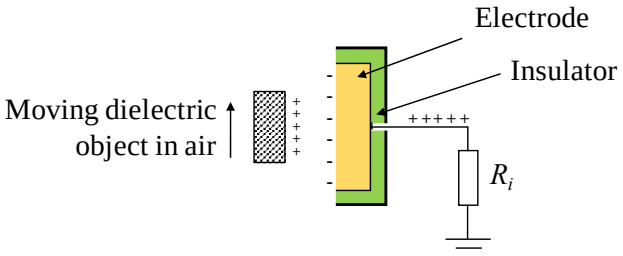

Fig. 1. Sensing of a moving non-conducting object through electrostatic induction.

Other terms such as ***electrodynamic*** have also appeared in the literature to describe the electric charging phenomenon. The word ‘electrodynamic’ is meant to stress that the charge is generated from the movement of a material with reference to another, bearing little relation to the actual sensing mechanisms, i.e. electrostatic induction or charge transfer. In fact, *electrodynamic effect* is concerned with the interaction between electric and magnetic fields. An *electrostatic* sensor entails the sensing principle is

electrostatic inductive or through charge transfer and has certainly no correlation with electromagnetic effect.

When a sensor works on electrostatic induction, the sensing principle may be explained in terms of an equivalent ***capacitive sensor***. This is because that the charged object can be modelled as a plate of a capacitor whilst the electrode itself is modelled as the other plate, as shown in Fig. 1. The movement of the charged object with reference to the electrode changes the distance between the two plates and hence the value of the capacitance. Similarly, the quantity of charge on the object may change with time and hence the voltage across the plates. This is why electrostatic induction is also termed as capacitive coupling in many references and thus an electrostatic sensor is equivalent to a capacitive sensor in such a case. In principle, both electrostatic sensors and capacitive sensors work on the fluctuation of the electric field around the sensing electrode. The fundamental difference between them lies in that the field fluctuation in an electrostatic sensor originates from the movement of a charged object, whereas the electric field in a capacitive sensor stems from an active electrode that creates the electric field and the object being measured modulates the (usually sinusoidally varying) electric field by varying the distance, electrode geometry or dielectric properties of the medium. These two types of sensor can have very different sensitivities, depending on the given application. For instance, electrostatic sensors are highly suited for the sensing of a dilute bulk material in a pneumatic suspension, but the capacitance types are normally applicable to heavily dense phase flow in a duct.

B. Electrode Design

A range of different electrode configurations have been used in commercial or prototype electrostatic sensors. Fig. 2 shows typical electrodes used to measure the characteristics of pneumatically conveyed solids in a pipe ((a)-(g)) and other processes such as a rotating shaft, human activity and burner flame ((h)-(j)). The physical size and shape of the electrode depend on the pipe dimensions and installation conditions. The shape and axial dimension of the electrode are the two key factors to be considered for a given pipe, as they affect the sensing volume, spatial filtering effect and spatial sensitivity [1]. An electrostatic sensor with a ring-electrode exhibits a major advantage over other types in that it is non-

restrictive to the movement of particles in a circular pipe. However, this feature is achieved at the expense of accommodating the electrode and insulator in a spool-piece with flanges. This limitation is less a problem for small pipe sizes (diameter < 300 mm), however, flanged spool-pieces with a large diameter can make the installation and future maintenance very difficult due to their heavy weight (see Section III.A). In contrast, intrusive sensors such as those shown in Fig. 2(e), (f) and (h) can be relatively installed by drilling holes on the pipes.

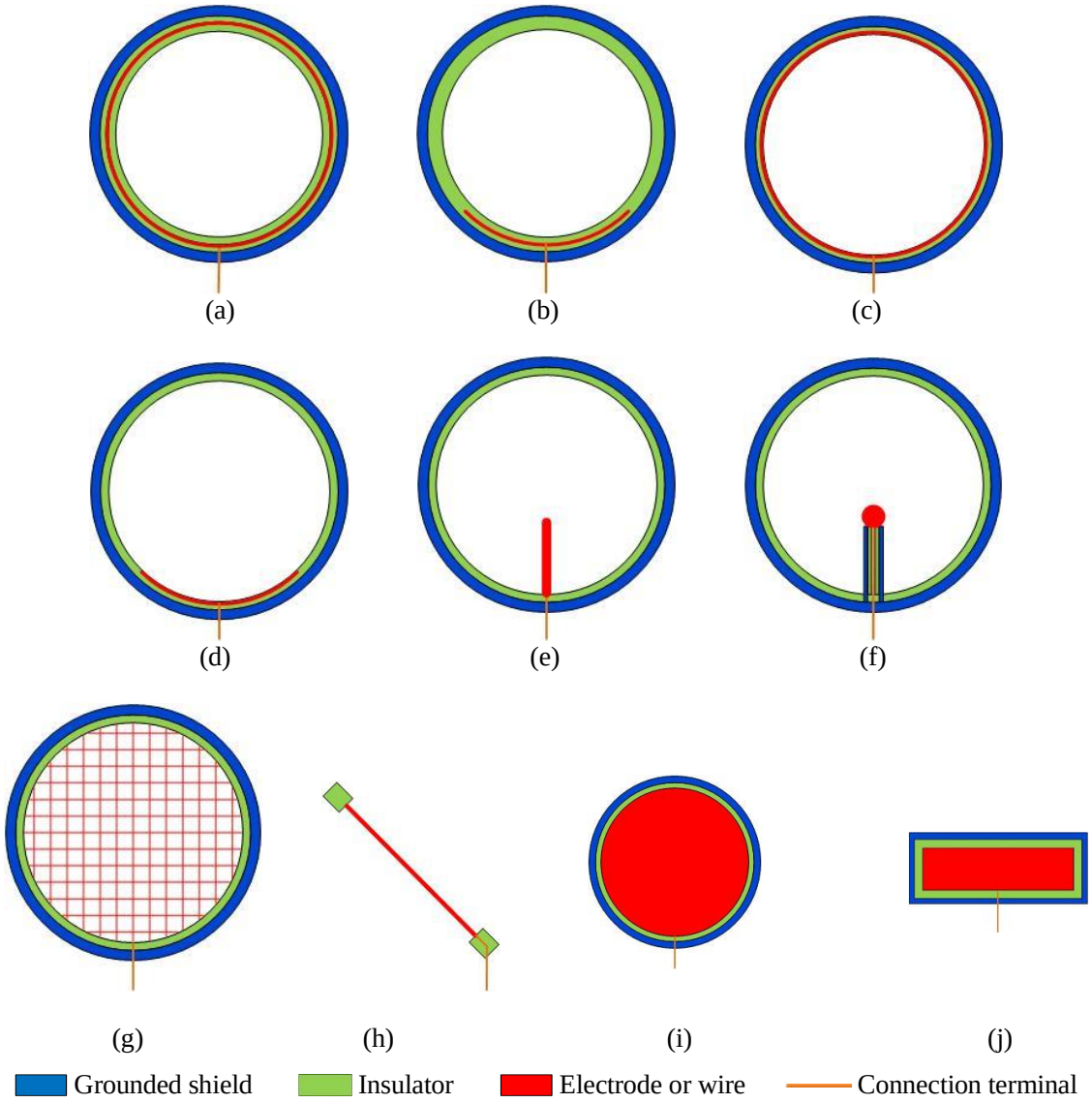

Fig. 2. Typical electrodes used in the measurement of particle flow characteristics ((a)~(f)) and other applications (g) and (j)). (a) Isolated ring. (b) Isolated arc. (c) Exposed ring. (d) Exposed arc. (e) Exposed/isolated rod. (f) Exposed ball. (g) Wire mesh. (h) Wire. (i) Disk or button. (j) Strip or plate.

In many applications an array of electrostatic sensors is often used to cover a specific sensing area of the target object or process being monitored. For instance, a number of exposed strip electrodes (Fig. 2(j)) can be used to sense the charged particles in a square shaped duct, such as those encountered in some

circulating fluidized beds and coal fired power stations. Fig. 3 depicts the different arrangements of the strip electrodes to cover the whole cross sectional area of the duct. Fig. 3(a) illustrates the simplest case where a single square shaped electrode has been used to acquire a signal without disturbing the flow in the square duct [2]. This single piece of square electrode can be readily split into four identical strip electrodes to detect the particles local to each of the electrodes (Fig. 3(b)). Furthermore, a matrix arrangement of 3x4 strip electrodes on the inner perimeter of the duct (Fig. 3(c)) enables the non-restrictive sensing of particles with a higher spatial resolution than that of the quadrilateral design [3]. Alternatively, a set of 3x3 strip electrodes arranged evenly across the square duct area (Fig. 3(d)) may be used to achieve a stronger spatial sensitivity for all particles, including those in the central area of the duct [4]. Such a specially designed sensing head is useful for the purpose of short-term experimental research, but is impractical for long term routine operation due to the abrasion of the electrodes by moving particles.

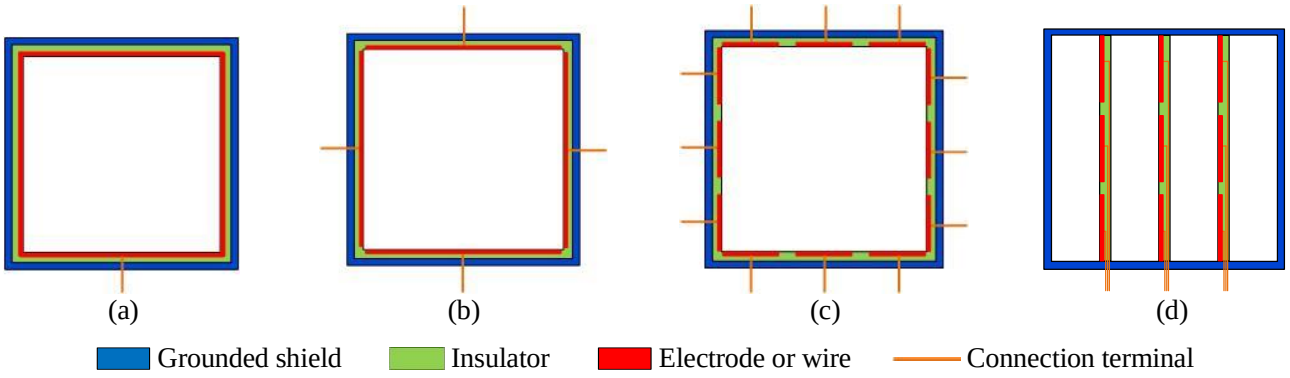

Fig. 3. Typical electrodes used in the measurement of particle flow characteristics in square-shaped pipes. (a) Single square. (b) Quadrilateral strips. (c) 3*4 strips. (d) Intrusive 3*3 strips.

It should be pointed that an array of electrostatic sensors is often arranged in the axial dimension to achieve an enhanced performance of the velocity measurement of pneumatically conveyed particles in a circular or square duct through data fusion [5].

C. Signal Conditioning Circuits

An inductive electrostatic sensor should be placed in a non-stationary electric field in order to obtain an output signal of some kind from the sensor. When the charge is static and the electric field remains constant, a time-varying electric field is usually produced by means of mechanical modulators such as rotating vanes of electric field mills [6] and micromachined resonators of MEMS (Micro-Electro-Mechanical System) electric field sensors [7]. In practice, the physical process to be monitored usually

involves some movement of a charged object that creates a varying electric field, which eliminates the need for mechanical modulators and simplifies the sensing system.

The signal conditioning circuit is an important element in an electrostatic sensor or sensing system. The circuit can be designed such that it derives only the alternating component (a.c.) of the sensor signal in a particular frequency range (a.c. method) or the direct component (d.c.) of the signal without concern over the frequency characteristics (d.c. method). In many cases the a.c. method outperforms the d.c. approach.

The signal conditioning unit usually consists of a pre-amplifier as the analog front end, a secondary amplifier for extra voltage gain and a low-pass filter for antialiasing or denoising. The pre-amplifier is the most important element because it not only determines the type of signal to be conditioned but also strongly influences certain key performance metrics of the circuit including stability, signal-to-noise ratio and, in some cases, the signal bandwidth. Since the original current or charge signal from the electrode is very weak, a high-performance pre-amplifier is essential. When the electrode is connected to a point with fixed electric potential either directly or via a resistor, the charge induced on or transferred to the electrode flows to that point. The charge signal is usually converted into a voltage signal using either a current conditioning circuit or a charge conditioning circuit. The electrode can also be left floating, such that its electric potential fluctuates in response to the movement of the charged object. In this case, an operational amplifier circuit with ultra-high input impedance should be utilised to buffer the electric potential signal.

1) Current conditioning circuits

Fig. 4 illustrates two simplified current conditioning circuits in shunt and feedback modes, respectively [8]. In both cases the electrode is modelled as a current source, suggesting that the variation rate of the induced charge is measured. In the shunt mode, the current I_S from the electrode flows to ground through the shunt resistor R_S and develops a voltage V_{in}, which is further amplified by the non-inverting amplifier. The voltage output is expressed as

$$V_O = I_S R_S (1 + \frac{R_2}{R_1}) \quad (1)$$

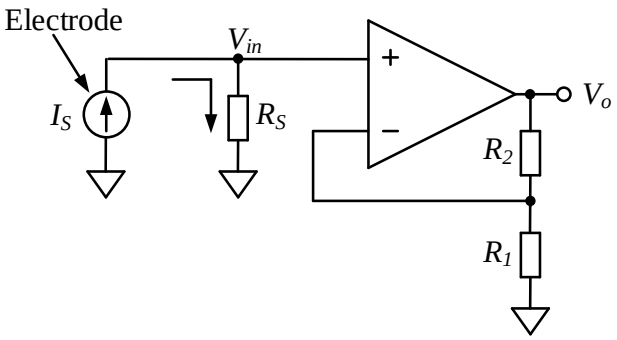

(a)

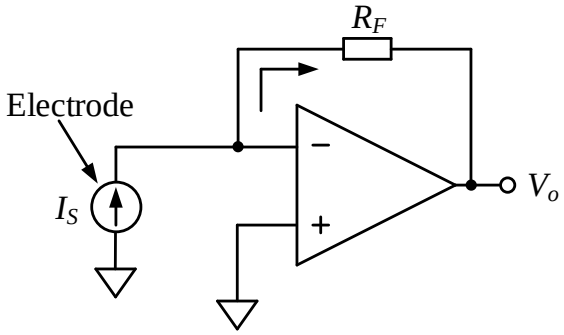

(b)

Fig. 4. Current conditioning circuits. (a) Shunt mode. (b) Feedback mode.

This circuit is less commonly used in comparison with the circuit in feedback mode, because its frequency response is affected by the stray capacitance of the electrode and the coupling capacitance between the electrode and the object being monitored.

The circuit in the feedback mode is also termed as transimpedance amplifier or current-to-voltage (I/V) converter. The electrode is connected to the virtual ground of the operational amplifier and the current I_S flows through the feedback resistor R_F to develop a voltage output expressed as

$$V_O = -I_S R_F \tag{2}$$

To achieve adequate sensitivity, a large value resistor R_F is commonly adopted. For sub-picoampere measurements, a T-shaped resistor network is usually utilised to substitute the feedback resistor with an extremely large value, which is unavailable or prohibitively expensive. A feedback capacitor may also be placed in parallel with R_F in order to ensure stability and limit the signal bandwidth.

The operational amplifier in both modes should have very low input bias current to reduce its impact on the electrode current. Special circuit design techniques such as guarding, shielding and Teflon insulation materials are also required to reduce leakage current which affects the quality of the sensor signal.

2) Charge amplifier circuits

Measurement of the total amount of the induced charge or transferred charge can be achieved using a charge amplifier in a quasi-static mode [9], as shown in Fig. 5(a). The electrode is connected to the virtual ground and modelled as a charge source Q_S. The induced or transferred charge on the electrode is stored in a feedback capacitor C_F. The voltage across the capacitor constitutes the output:

$$V_O = -\frac{Q_S}{C_F} \tag{3}$$

A reset switch in the form of a relay or a junction field effect transistor (JFET) is utilised to discharge the feedback capacitor and bring periodically the output voltage to zero to prevent the charge amplifier from entering saturation. Quasi-static charge amplifiers are standard conditioning circuits of Faraday pails and provide information about the polarity of charge on the object being measured.

When only the variation rather than the total amount of the charge is concerned, a charge amplifier working in an AC mode that substitutes the reset switch with a feedback resistor can be used for dynamic measurement, as shown in Fig. 5(b). The feedback capacitor is continuously discharged via the feedback resistor at low frequencies to prevent the amplifier from drifting into saturation. The resistor also provides a DC negative feedback of the output. It is worth noting that the circuit in Fig. 5(b) appears deceptively as a low-pass filter, but in fact it is a high-pass filter as charge Q_s is now the input instead of the usual voltage input [10]. To enhance the frequency response of the circuit, the feedback resistor should be sufficiently large.

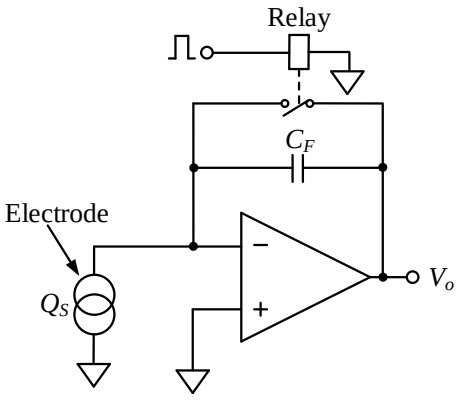

(a)

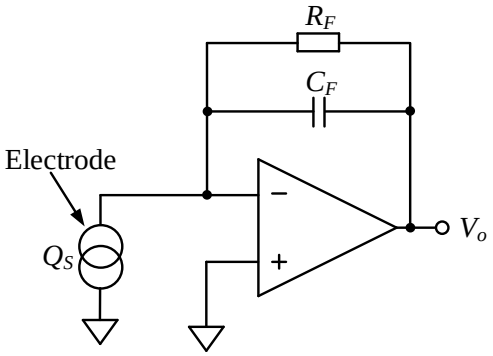

(b)

Fig. 5. Charge conditioning circuits - charge amplifiers. (a) Quasi-static mode. (b) AC mode.

3) Electric potential measurement circuits

If the measured object and the electrode are modelled as two plates of a capacitor, the electric potential of the electrode can be measured using a unity gain buffer amplifier [11], as shown in Fig. 6. The electrostatic voltage of the charged object can be represented by V_S and the coupling capacitance between the measured object and the electrode is denoted as C_S. The high source impedance requires an amplifier with ultra-high input impedance in order to avoid signal attenuation and to minimise dependence of the gain on the coupling capacitance. However, a grounded resistor R_B that degrades the input impedance is necessary to provide a path for the bias current of the amplifier. In addition to the bias resistor R_B, the source voltage V_s is also divided by the stray capacitance C_x of the circuit board and the input capacitance C_{in} of the amplifier, as illustrated by the following expression of the input voltage V_{in}

$$V_{in} = \frac{j\omega R_B C_s}{1 + j\omega R_B (C_{in} + C_x + C_s)} Vs \tag{4}$$

Several techniques have been reported in the published work to enhance the sensitivity of the signal conditioning circuit, such as bootstrapping to increase the input resistance, neutralisation and active guarding to reduce the capacitance at the non-inverting terminal of the operational amplifier [11]. In some papers [11], [12], the term electric potential sensor has been used to describe the sensing technique when such a signal conditioning circuit is adopted.

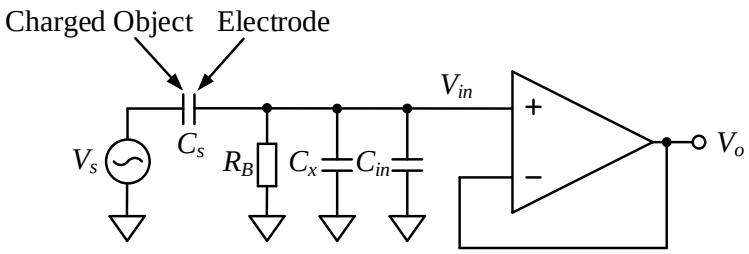

Fig. 6. Circuit for electric potential measurement.

D. Signal Processing Algorithms

A range of signal processing algorithms have been developed and utilised along with electrostatic sensors over the years. Signals from many electrostatic sensors are often stochastic due to the random nature of the process or system being monitored. Some processing of the signals is straightforward such as the determination of parameters of time domain or frequency parameters. For example, the Root Mean Square (RMS) value of the signal from an electrostatic sensor is often used to represent the magnitude of the signal. The RMS value of the signal is defined as

$$V_{rms} = \sqrt{\frac{1}{N}\sum_{k=1}^{N} S^2(k)} \tag{5}$$

where $S(k)$ ($k = 1, 2, \ldots, N$) represents the sampled signal $S(t)$ and N the number of data samples available in each measurement cycle.

For a sensor signal its energy and power are also useful characteristic variables or features in the time domain in some applications. These are defined as

$$E = \sum_{k=1}^{N} S^2(k) \tag{6}$$

$$P = \frac{1}{N}\sum_{k=1}^{N} S^2(k) \tag{7}$$

where E and P represent the energy and power of the signal $S(t)$, respectively.

In some applications signals from some electrostatic sensors contain a periodic component due to the repetition of the process or system being monitored, e.g. rotational motion of a shaft (Section III.C). The periodicity of the signal from an electrostatic sensor can be determined through autocorrelation

processing. The period of the signal (*T*) can be determined from the location of the dominant peak in the autocorrelation function *R(m)*, which is defined as

$$R(m) = \frac{1}{N}\sum_{k=1}^{N} S(k)S(k+m) \tag{8}$$

where *N* is the number of data samples in the correlation computation and *m (m=0, …, N)* is the number of delayed points. Note that the autocorrelation function with no delay points (i.e., *m*=0) equals to the signal power *P* (equation (7)). To avoid zero padding in the delayed signal *S(k)* during correlation computation, the total number of data points in each processing cycle should be 2*N*. A normalised version of the autocorrelation function is often used to obtain correlation coefficient, i.e.

$$\rho(m) = \frac{\sum_{k=1}^{N} S(k)S(k+m)}{\sum_{k=1}^{N} S^2(k)} \tag{9}$$

The term, correlation coefficient, is the magnitude of the dominant peak in the normalised autocorrelation function other than the unity at *m*=0. Correlation coefficient represents, to some extent, the reliability of the measurement through autocorrelation. The autocorrelation function of a signal reveals its internal structure in the time domain and whether it contains a periodic component. The correlation coefficient indicates the degree of periodicity in the signal waveform. The location of the dominant peak on the time axis indicates the period *T*. Fig. 7 shows a typical example of a periodic random signal and the resulting autocorrelation function.

In many practical applications a pair of identical electrostatic sensors is often used to measure the speed of a target in either linear or circular motion of an object or a cloud of small objects such as particles in a duct. In such cases the two signals are similar in nature, but there is a short time delay between them due to the physical linear or angular spacing between the sensors that detect the movement of the target. The time delay can be determined through cross-correlation of the two signals, which is defined as

$$\rho_{12}(m) = \frac{\sum_{k=1}^{N} S_1(k)S_2(k+m)}{\sqrt{\sum_{k=1}^{N} S_1^2(k)}\sqrt{\sum_{k=1}^{N} S_2^2(k)}} \tag{10}$$

where $S_1(k)$ and $S_2(k)$ $(k = 1, 2, \ldots, N)$ are the sampled version of the signals $S_1(t)$ and $S_2(t)$, respectively. The time shift corresponding to the dominant peak in the cross-correlation function is the time delay between the two signals. Fig. 8 illustrates two typical signals from a pair of electrostatic sensors and resulting cross-correlation function where the time delay (τ) between the two signals is shown on the time axis. The value of the dominant peak represents the similarity between the two signals, which is an indication of the reliability of a correlation velocity measurement system.

Other signal processing techniques such as power spectral density analysis, wavelet transform and Hilbert-Huang transform are common methods used in the processing and analysis of signals from electrostatic sensors. In some applications a wide variety of features are extracted from a sensor signal in the time domain, frequency domain or time-frequency domain through a combination of several signal processing methods. Further details of the signal processing algorithms used in specific applications of electrostatic sensors are given in Sections III and IV.

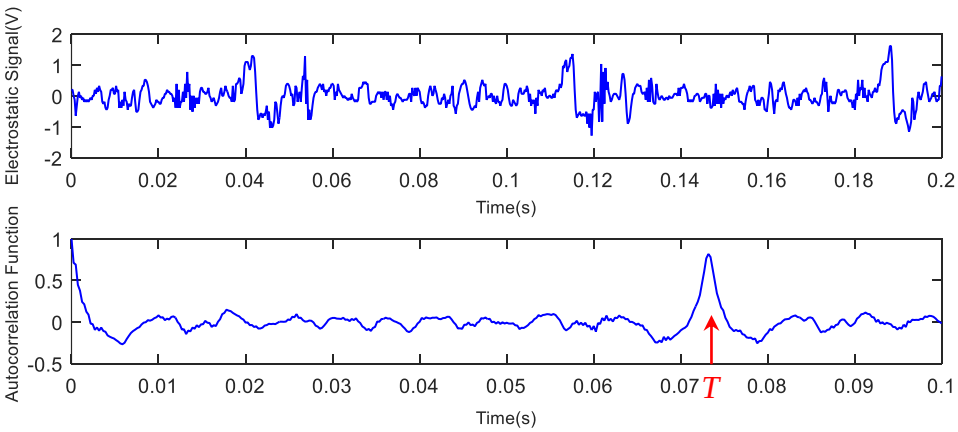

Fig. 7. Typical periodic random signal and resulting autocorrelation function [13]. Copyright © 2015, IEEE

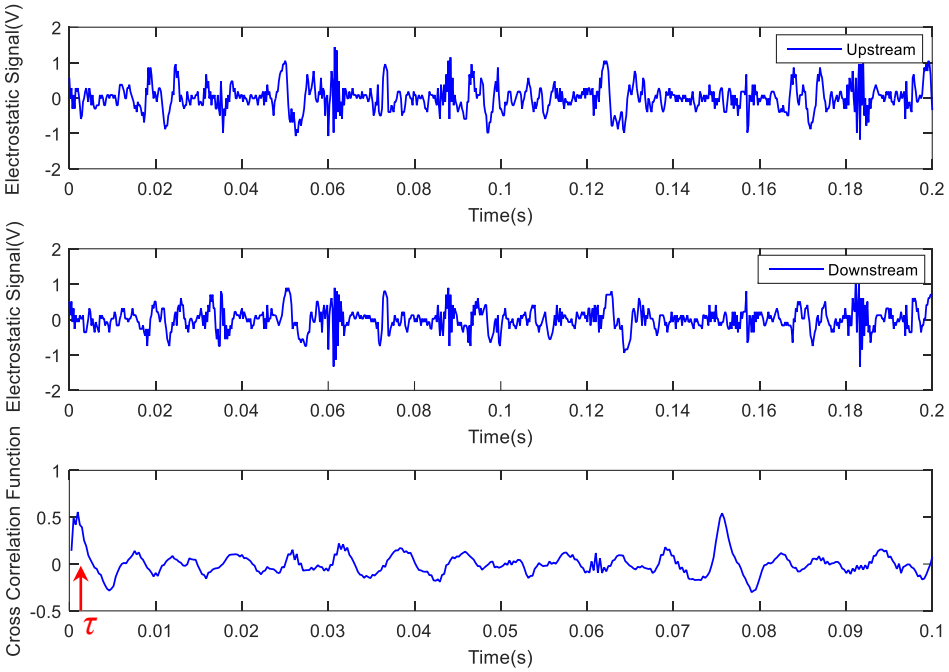

Fig. 8. Typical signals from a pair of electrostatic sensors and corresponding cross-correlation function [13]. Copyright © 2015, IEEE

III. APPLICATION

A. Flow Measurement of Pneumatically Conveyed Solids

The pneumatic transportation of bulk solids through enclosed pipes has been widely adopted in many industrial processes. The key dynamic characteristics of solids in a gaseous stream are essential for the optimisation of solids conveying processes and operational parameters of related equipment to achieve better product quality, greater productivity and efficient utilisation of energy. However, the distribution of solids in a pipe is highly inhomogeneous whilst the velocity profile of particles over the pipe cross section can be highly irregular. This difficult nature of solids flow often leads to fluctuations in the measured particle flow parameters or even spurious readings, which are out of a reasonable range. The on-line measurement of pneumatically conveyed solids has long been recognised as a technically challenging area.

Over the past few decades, enormous effort has been spent on the development of suitable techniques which may offer practical solutions to the measurement of solid particles in pneumatic pipes. The direct methods such as those based on impact plates [14] are inherently not suitable as they always require interception of the flow and suffer from wear and blockage problems. Most of the available inferential methods [14],[15] using electromagnetic waves (from γ-rays to microwaves), digital imaging, optical,

thermal, ultrasound, electrical capacitance and mechanical vibration techniques, however, are less practical or industrial applicable but more scientific and laboratory orientated due to their intrinsic limitations [15]. Solid particles in a pneumatic pipe are charged due to the triboelectric effect (Section II.A) [16]. Although triboelectric electrification of solids is a hazardous phenomenon that undermines the safety of industrial processes, electrostatic sensors make good use of it to measure the characteristics of pneumatically conveyed solids. The exact level of charge on the particles is difficult to predict, however, it can be detected with an electrode together with an electronic circuit (Section II.C). Because the sensors are sensitive only to the particles in motion, the signals are little influenced by the physical properties and accumulation effect of solids in the pipe, which adversely affect other sensing technologies [15]. In recognition of the advantages of good affordability, simple structure, passive measurement (i.e., no injection of energy in any form to the flow medium), minimum maintenance and stable performance, extensive modelling and experimental studies of a variety of electrostatic sensors with different shapes and sizes of electrodes [17], [18] have been conducted. Generally, intrusive sensors [19] provide stronger signals than non-intrusive ones, but suffer from wear problems and are prohibited in many industrial applications. An arc-shaped electrode [5], [20] is sensitive to the movement of particles close to it and is thus suitable for measuring localised characteristics of solids in an inhomogeneous flow regime when several electrodes pairs are installed around the pipe perimeter. The ring-shaped electrode [1], [20]–[23] is the most common one that exhibits better performance over other types as its sensing area covers the whole cross section of the pipe, giving cross-sectionally averaged flow parameters [9].

The signals from electrostatic sensors [9], [25] are a source of information about the flow parameters of solids, of which the velocity and volumetric concentration are two basic and the most important ones. Cross-correlation velocimetry [1], [22] is a well-established statistical method to determine the particle velocity in a pneumatic conveying pipe. An electrostatic sensor also offers the most simplest and cost-effective means of measuring the relative volumetric concentration of solids among all proposed techniques [15]. The main problem in applying the electrostatic sensing principle is to relate the concentration to be measured to the magnitude of the sensor signal, which depends upon the physical properties of particles (e.g. size, shape, velocity, permittivity and chemical composition) and flow

conditions (e.g. pipe diameter, wall roughness, line temperature and humidity) [9], [16], [17], [26]. The RMS charge magnitude is adopted to indicate relative concentration of particles under steady flow conditions [5], [9], [16]. Because flow conditions in some industries are mostly dilute and steady, the RMS level can be regarded as being proportional to the solids concentration [1], [14].

The mass flow rate of solids is another key parameter to be derived from the measured particle velocity (v_c) and volumetric concentration of solids (β_s) according to the following equation [9], [26]:

$$q_{m,s} = A_p \rho_s v_c \beta_s = a v_c^b A_{rms} \tag{11}$$

where A_p is the cross-sectional area of the pipe, ρ_s is the true density of solids, a is a constant depending on the properties of solids, A_{rms} is the RMS amplitude of the sensor signal, and coefficient b represents the dependence of A_{rms} on flow pattern and particle velocity. It should be stressed that particle velocity affects the RMS level as it determines the extent of the triboelectric effect in the pneumatic conveying pipe. The higher the particle velocity, the more electrostatic charge is generated on particles [26]–[28]. Coefficients a and b are determined through calibration with reference data from isokinetic sampling equipment. The particle velocity and solid distribution (or profile) in the pipe cross section can also be obtained using an array of electrostatic sensors [23], which normally consist of a number of identical strip-shaped electrodes across the cross section of the pipe.

Although there still exist some technical issues, such as the non-uniformity in the sensitivity of electrostatic sensor [29], dependence of the RMS amplitude on environmental conditions and particle properties [26], etc., the electrostatic sensing technique has been widely used in many industries in recent years. One successful deployment is the application on fuel feeding pipes on pulverised fuel (PF) fired power plants [27], [28]. PF fired power stations face substantial challenges to maintain economic viability and comply with increasingly stringent emission regulations. Solid fuels are pulverised into small particles and then injected towards a set of burners via a network of pipes. On-line continuous measurement of fuel flow parameters in the fuel pipes allows the plant operators to control and optimise the fuel supply and to detect problems such as oscillations or roping flow (even pipe blockage [30]) at an early stage, particularly when changing the fuel diet and operating conditions. In view of the complex dynamic behaviours of the PF particles in large diameter pipes, a measurement system with a set of electrostatic sensor arrays and a

data fusion algorithm is developed to enhance the measurement performance. Fig. 9(a) shows three identical narrow electrodes and one wider electrode to obtain the sensor signals. The narrow electrodes are used to measure the PF velocity through multi-channel correlation by permutation of the signal pairs. Fig. 9(b) shows a typical example of the three signals and resulting correlation functions obtained from on-plant trials. The measurement system should still be functioning if one of the sensors is faulty or no valid measurement is available from one or two pairs of the signals under complex flow conditions due to an ill-defined correlation peak. The weighted average PF velocity is finally determined by combining the three individual velocities [20], [27]. The wider electrode, which has better spatial filtering effect and a larger sensing volume [1], [21], is utilized to measure the RMS charge level of PF for the determination of the mass flow rate from equation (11).

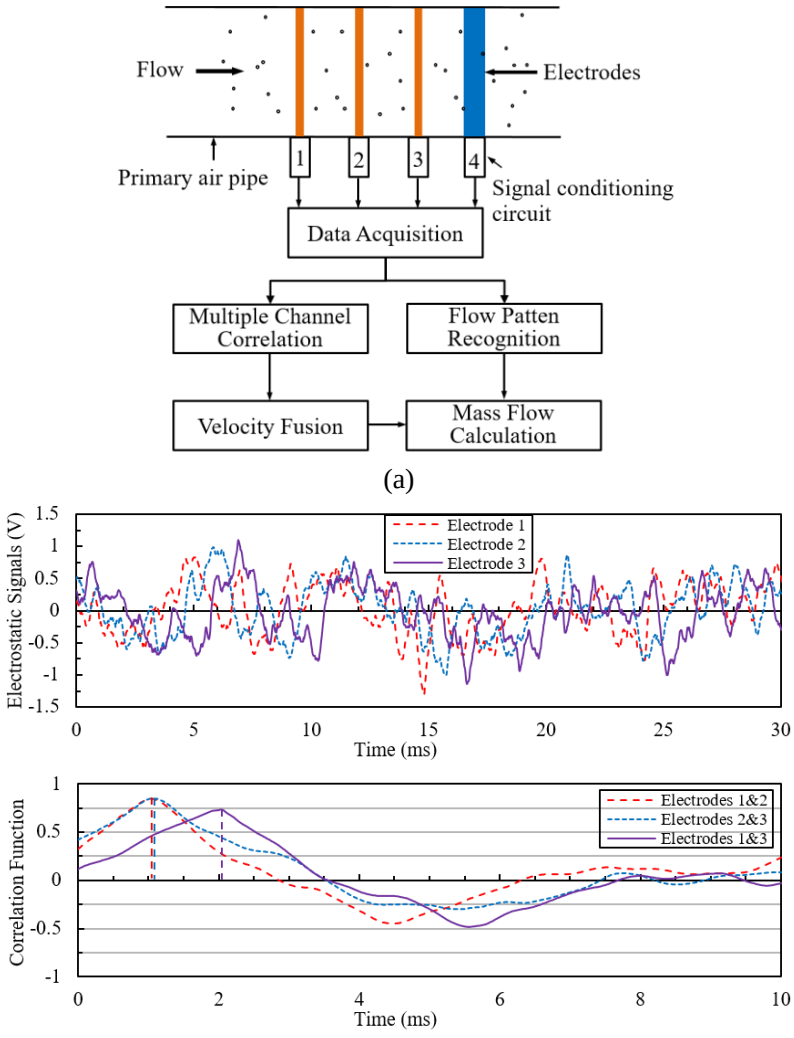

Fig. 9. Principle of the PF flow measurement system and typical signals. (a) System structure. (b) Typical signals from electrostatic sensors and resulting correlation functions [27], [28]. Copyright © 2017, IEEE Copyright © 2014, Elsevier

In most industrial applications the sensing heads need to be installed on the pipes without any intrusiveness to the flow. In this case, ring-shaped [27] and arc-shaped [28] electrostatic sensor arrays are preferred as they measure cross-sectionally averaged and localised fuel flow parameters, respectively. Fig. 10 shows a typical example of a five-sensing-head system with ring-shaped electrodes on the pulverising mill of a 1000MW furnace for 7/24 operation. In order to determine the fuel distribution between the five PF pipes from the same mill, all the components of the sensing heads are made identical to each other. The measured flow parameters are transmitted to an on-site central data analysis station. The data are also transmitted to the distributed control system (DCS) at the plant, enabling the automatic control of the fuel milling and injection process. The long-term operation of the measurement system since its installation has generated important data for the plant operators, demonstrating that the system is capable of measuring the PF flow and distribution between the fuel pipes from the same pulverizing mill. The on-plant performance of the system has been validated using the well-established isokinetic sampling equipment [27]. The discrepancy between the PF and the primary air velocities is found to be below 4%. The relative error in the fuel flow distribution measurement with reference to that from the isokinetic sampling equipment is within ±13%. The deployment of the PF flow measurement system has generated significant benefits, including better control of the pulverizing mill, increased process efficiency and reduced pollutant emissions. A range of commercial solids flow instruments based on electrostatic sensing are now available on the market.

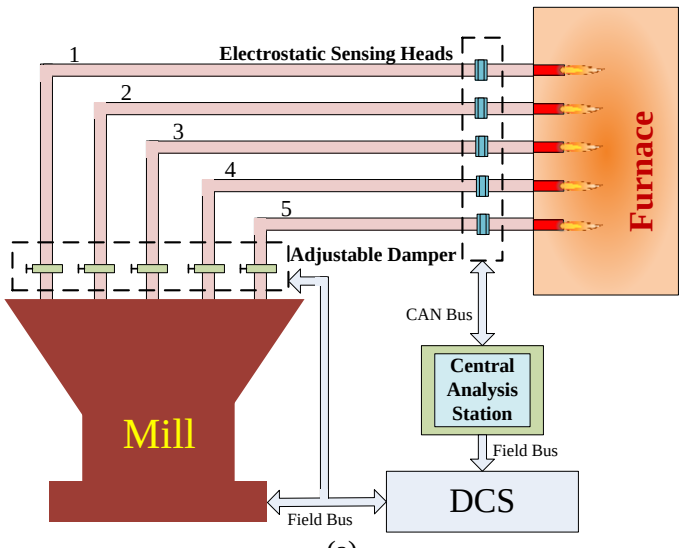

(a)

(b) (c)

Fig. 10. Application of the PF flow measurement system with five electrostatic sensing-heads. (a) Schematic of the measurement system on a furnace. (b) Installation of the electrostatic sensing head. (c) A set of four sensing heads on the same pulverising mill [27]. Copyright © 2017, IEEE

B. Measurement of Particulate Emissions

On-line continuous measurement of particulate emissions from industrial processes is essential to achieve effective emission control and reinforce environmental regulations [31]. The main technologies for the monitoring of particulate emissions include light scattering, optical attenuation, radiation absorbency and triboelectric sensing. Electrostatic sensors offer a practical solution to the on-line continuous measurement of particulate emissions in terms of mass concentration and mass emissions [14].

Particulate solids in industrial flues and chimneys carry electrostatic charge due to the relative motion between the particulates and the gas stream as well as the actual industrial process, e.g. coal combustion process which generates the particulates. A grounded sensor rod is inserted into the stack to detect the fluctuations of the transferred charge due to the passing and colliding of particles with the rod.

In this case the a.c. method usually outperforms the d.c. method in terms of repeatability. The signal conditioning unit filters out the unwanted d.c. component in the sensor signal and derives the a.c. component within an optimised frequency bandwidth. The RMS magnitude of the signal, which is found independent of the rod surface condition, has a stable and repeatable relationship with the mass concentration of particulates in an industrial stack [33]. Based on this design approach several products have been available on the market for mass concentration measurement for several decades. Such products have been improved incrementally over the years either in the signal conditioning electronics or signal and data processing software. The probe-type electrostatic sensor, as shown in Fig. 11, incorporates an auto-

gain-control mechanism, enabling the monitoring of mass concentration of particulates from 0.05 mg/m^3 to 1000 mg/m^3 in stacks from 0.2 m to 4 m [33]. It is worth noting that the electrostatic sensing method is capable of detecting a wider range of dust concentrations than that of the optical opacity approach. The lower limit of the opacity monitors is around 10-30 mg/m^3 [33].

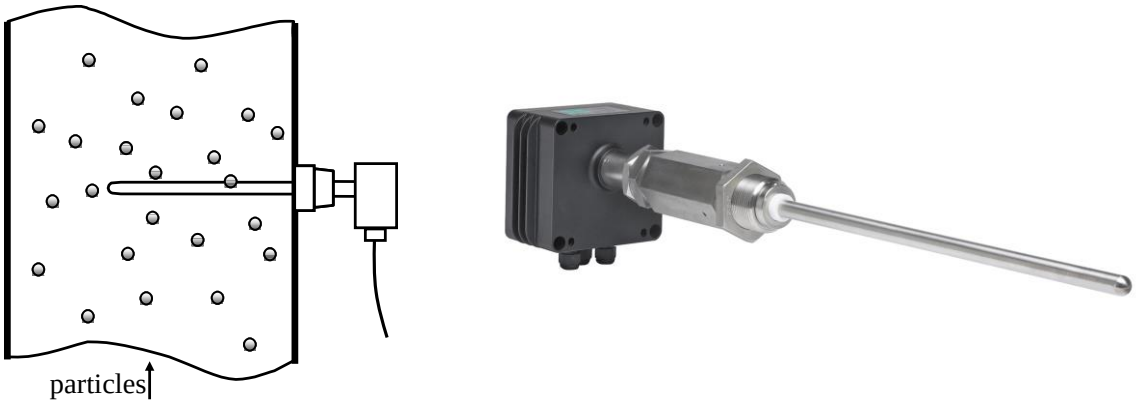

(a) (b)

Fig. 11. Monitoring of particulate mass concentration. (a) Sensing arrangement. (b) Example product [31]. Copyright © 2005, IEEE

The electrostatic method for mass concentration monitoring has a clear shortcoming in that the sensor output signal depends on a range of other factors, such as properties of the particulates, environmental conditions in the duct, velocity of particulates etc. A mass concentration monitor operating on the electrostatic sensing principle may be calibrated with particles of known physical properties under steady stack flow conditions. However, variations in the actual particulates and their flow conditions may lead to large errors in mass concentration measurement. This also means it is difficult to interpret the RMS amplitude of the sensor signal in terms of mass concentration of particulates. It is because of this limitation that some manufacturers indicate their particulate monitors are effective for trending and relative comparison such as in processes where moisture may fluctuate significantly instead of providing absolute mass concentration measurement.

For the purpose of particulate emission monitoring, the mass emission represents a practical measurement of particulates actually emitted into the atmosphere. In order to determine the mass emission of particulates (q_m) in g/s, the velocity of particulates needs to be measured independently, i.e.

$$q_m = 10^{-3} A \, v \, \beta_m \tag{12}$$

where A is the duct cross sectional area in (m^2) and v and β_m are the velocity (m/s) and mass concentration (mg/m^3) of particulates, respectively.

The velocity of particulates can be measured through correlation velocimetry. A pair of electrostatic sensing probes is installed (Fig. 12) on the stack. The transit time taken for the particulates to travel from the upstream probe to the downstream one is determined from the cross-correlation function between the two sensor signals. The velocity (v) is calculated from the known sensor spacing (L) between the sensing probes and transit time (τ):

$$v = \frac{L}{\tau} \tag{13}$$

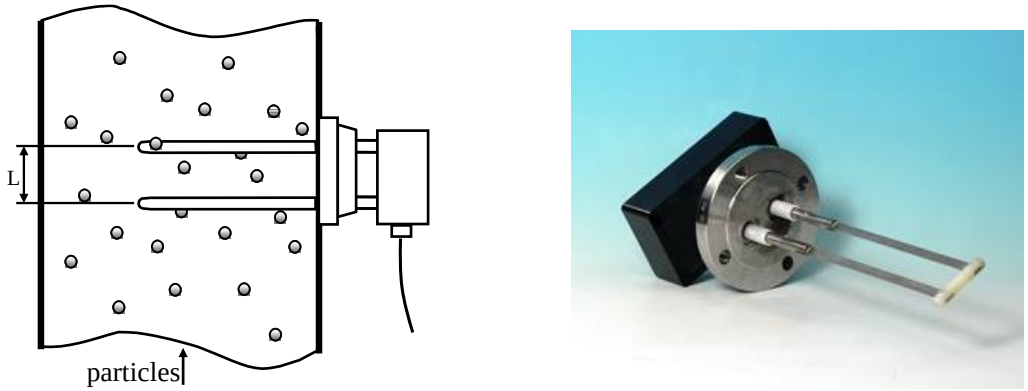

(a) (b)

Fig. 12. Cross-correlation particle velocity measurement. (a) Sensing arrangement. (b) Photo of the sensor [31].

Since cross-correlation velocimetry measures the time delay between the two signals, the velocity measurement does not depend on the signal amplitude. This means the velocity measurement is independent of the particulate properties and stack conditions. It must be pointed out that this technique measures the actual velocity of particulates rather than the velocity of the gas stream in a stack such as those based on thermal anemometers, ultrasonic transceivers or Pitot tubes. This particular feature is regarded as important since solid particles can move up in a stack at different velocities from the gas phase.

Electrostatic sensor based dust monitors have been successfully deployed to detect low particulate emissions (in the order of 1 mg/m^3) after dust filtration systems in some industrial sectors [33]. Since the velocity of particulates is also a key factor that adversely affects the mass concentration measurement,

the dust monitors are optimised to minimise the influence of the velocity of particulates over a narrow range, typically from 10 to 20 m/s.

It is impractical to quantify the accuracy of the velocity measurement system without available standards. However, the repeatability of the measurement system has been found to be better than 2% with non-linearity within ±1% [34]. The velocity measurement system works on the principle that the two signals from the sensors are sufficiently similar. This means the dust level in the stack must be over a particular threshold to obtain a reliable velocity measurement. The threshold, i.e. the lower limit of the mass concentration of particulates, has been found to be dependent upon the type and velocity of particulates. The threshold can go below 0.1 mg/m^3 for the higher velocity range (>10 m/s). This implies that the minimum mass emission per square meters is approximately 1 mg/s (equation (12)). The probe-based dust monitors can normally be installed on stacks ranging from 50 mm to 6 m in diameter [33]. Such monitors are little affected by probe contamination due to build-up of dust particles and are capable of detecting wet or aggressive particulates at temperatures as high as 800°C.

The electrostatic sensing technology incorporating digital signal processing algorithms, despite its limitations, offers a simple and cost-effective solution to measuring the mass concentration, velocity and mass emissions of particulates in industry. Dust monitors operating on the electrostatic sensing principle are now widely deployed in numerous processes across all industrial sectors.

C. Monitoring of Fluidised Beds

Due to the excellent heat and mass transfer capabilities, gas-solid fluidised beds are widely used in various industries, such as catalytic cracking of petroleum, polymerisation, combustion and gasification, food processing and pharmaceutical industries. However, the design, scaling up and control of fluidised beds rely significantly on experience [35]. As a result, techniques for the monitoring of particle hydrodynamics in fluidised beds are necessary. Sun and Yan conducted a review of techniques for the measurement and hydrodynamic characterisation of gas-solid fluidised beds [35]. Various non-intrusive methods have been developed to measure global and local flow parameters. These include Acoustic Emission (AE) detection, imaging, tomography, particle-tracking, Laser Doppler Anemometry (LDA)

and Phase Doppler Anemometry (PDA), and pressure-fluctuation methods. Taking the characteristics of low cost and real-time measurement into account, they pointed out that electrostatic sensors should be preferentially considered for the monitoring of fluidised beds.

Electrostatic charging is inevitable in fluidised beds due to triboelectric effect. Several review articles have been published to focus issues on the charge generation and distribution, relationships between the electrostatic phenomenon and hydrodynamics, and electrostatic charge control [36]–[38]. In addition to investigations into electrostatic phenomena in fluidised beds, useful information for the condition monitoring of fluidised beds can be obtained by processing the signals from electrostatic sensors. Applications of electrostatic sensors to fluidised bed monitoring are presented in the following sections.

1) Characterisation of heterogeneous flow structure

The heterogeneous phase distribution, flow regime fluctuation, variations in the velocity and acceleration of solid and gaseous phases as well as variable operational conditions make the flow structure in a fluidised bed very complex. The signals from electrostatic sensors contain useful information about the heterogeneous flow structure in a fluidised bed. The velocity and relative concentration of solids can be characterised by processing the signals. Zhang *et al.* [39] proposed a proof-of-concept design to monitor the flow dynamics in a triple-bed combined circulating fluidised bed (CFB) through the combination of an electrostatic sensor and a twin-plane electrical capacitance tomography (ECT) sensor over a wide range of flow regimes. The solids velocity was estimated by cross-correlating the signals from the upstream and downstream electrostatic sensors. A homogeneous flow regime was observed with an almost flat velocity profile of solid particles with a dilute suspension flow in the riser. On the contrary, the flow becomes inhomogeneous in the downer and the solids velocity in the centre of the downer is higher than that near the wall. Electrostatic sensors can also be applied to characterise the flow dynamics in a bubbling fluidised bed [40], [41]. The experimental set up is illustrated in Fig. 13. Several sets of electrodes with four arc-shaped electrodes in each set were tightly wrapped on the outer wall of the fluidised bed. The electrodes were positioned strategically on the fluidised bed in order to obtain information on the behaviors of particles in different local areas of the bed. The velocities of Geldart B

and D particles were measured and analysed. Due to the dominant bubble split over coalescence, the bubble size was smaller for Geldart D particles and a less number of bubbles were formed under the same excess gas velocity. As a result, the average velocity of Geldart D particles was significantly smaller than that of Geldart B particles. Sun and Yan [42], [43] applied arc-shaped electrostatic sensors to characterise the coherent structure and clusters in the riser of a CFB, in addition to the velocity and relative concentration of solids. Through a comparison of the extended self-similarity scaling law curves before and after the extraction, the effect of coherent structures on the flow intermittency was observed, suggesting that the signals contain useful information about the intermittent hydrodynamic behaviors of particles in the bed [42].

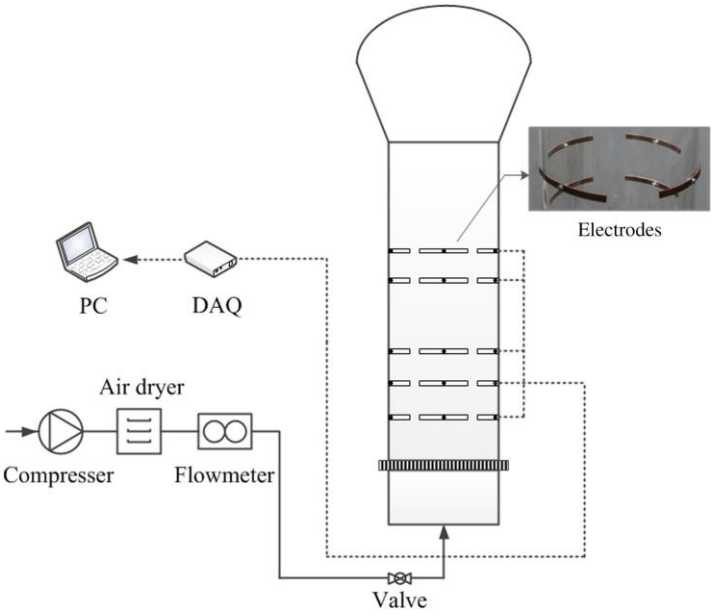

Fig. 13. Experimental apparatus with electrodes [41]. Copyright © 2017, Elsevier

2) Characterisation of electrostatic charge

In addition to the direct method with a Faraday cup, indirect method of electrostatic probes and sensors are widely applied to characterise the electrostatic charges in fluidised beds. Unlike the Faraday cup, which is a static measurement tool, the signals from the electrostatic sensors contain dynamic information on particle charging and hydrodynamics inside a fluidised bed. Zhang *et al*. [44] used wire-mesh electrostatic sensors to monitor the charge distribution in a bubbling fluidised bed. Compared to other electrostatic sensors, wire-mesh sensors exhibit higher and more uniform sensitivity distribution. The charge distribution across the cross section of the fluidised bed was reconstructed from the induced

charge on the electrodes and sensitivity distribution of the sensors. Experimental studies were carried out on a bubbling fluidised bed under laboratory conditions (Fig. 14). It was found that the charge distribution in the dense phase region is relatively uniform and that in the splash region is significantly affected by the flow dynamics. However, wire-mesh sensors are intrusive to the particle flow in the bed and an online calibration is required to obtain the induced charge on the electrodes. Moreover, electrostatic sensors installed outside the bed were also used to measure the charge density and its effect on particle motions in a bubbling fluidised bed [45], [46]. Ring-shaped electrodes and a pressure sensor, together with a modified model which considers the effect of the spatial sensitivity of the sensing electrodes were employed to predict the particle charge density [45]. Shi *et al.* [46] proposed an array of arc-shaped electrostatic sensors to simultaneously measure the electrostatic charge and its effect on particle motion in a fluidised bed. Through the analysis of induced sensor signals, particle velocity and charge-to-mass ratio of particles under different charging levels, a model for predicting the average charge-to-mass ratio was also established. It should be noted that the aforementioned models are only applicable to certain conditions in either case, thus for a wide applicability new models that consider the sensing mechanism and physical principle of the process being monitored are desirable. Finally, considering the intrusive probes, He *et al.* [47], [48] developed a dual tip electrostatic probe to measure concurrently the in-situ charge density of particles and the size and rise velocity of bubbles. Several decoupling methods were proposed to analyse the signals from the probes. The charge density and bubble rise velocity were found to follow the same trends as those from a Faraday cup system and a video imaging system, respectively. Although the results are encouraging, intrusive probes can only obtain the charge distribution in a specific region of the fluidised bed.

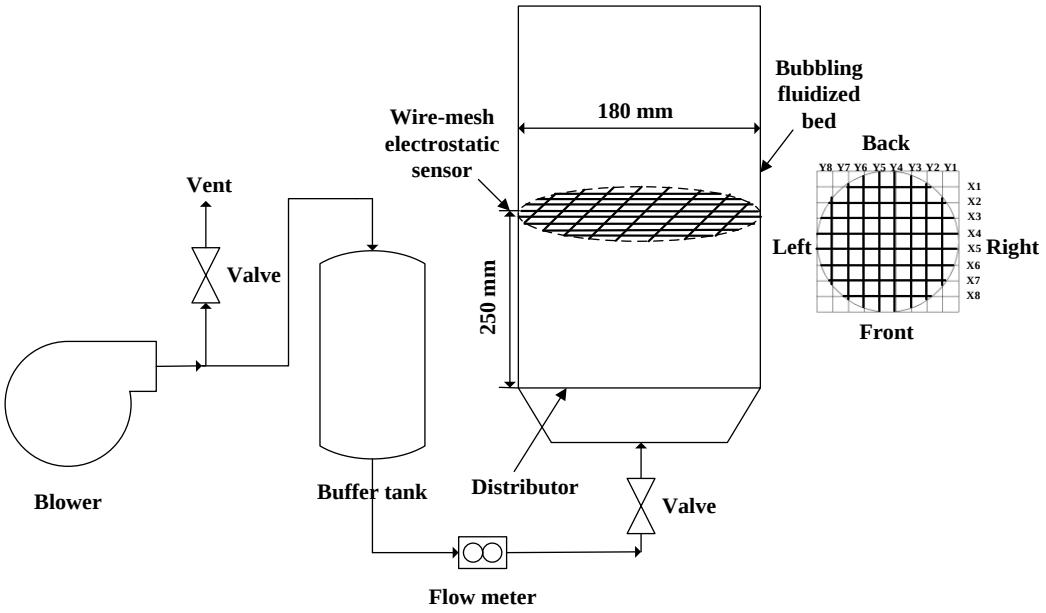

Fig. 14. Experimental setup of the wire-mesh sensor in a bubbling fluidised bed [44]. Copyright © 2017, IEEE

3) Measurement of moisture content

Fluidised bed dryers (FBDs) are widely deployed to dry up raw materials or final products because of the high efficiencies in mixing and mass and heat transfer. To control and optimise the operating process of a FBD, it is necessary to monitor the moisture content of particles in the bed. The charge on the particles is a direct indication of the moisture content, so the signal due to the fluctuations of the charge is used to monitor the drying process. Zhang *et al*. [49] conducted experimental investigations on the moisture content measurement of biomass using an electrostatic sensor array. It was found that the variability of the sensor signal indicates the change in moisture content. However, the air velocity had a significant impact on the relationship between the RMS magnitude of the signal and the moisture content. By taking the velocity effect into account, an empirical predictive model for moisture content measurement was established with the average RMS magnitude. Predicted values using the signals from the sensor array are within ±15% of the reference moisture content. In order to further improve the accuracy of moisture content measurement, a machine learning model based on random forest (RF) algorithm was proposed [50]. The features of sensor signals in the time and frequency domains, particle velocity and the outlet temperature and humidity of exhaust air from the FBDs were chosen to be the input vector of the RF model, as shown in Fig. 15. The hyper-parameters of the RF model were tuned using the Bayesian optimisation algorithm. In addition, online prediction of the moisture content in a lab-

scale platform was conducted with the experimental condition beyond the range of the training data. The online prediction results follow the trend of the sampled results with a relative error within 13%.

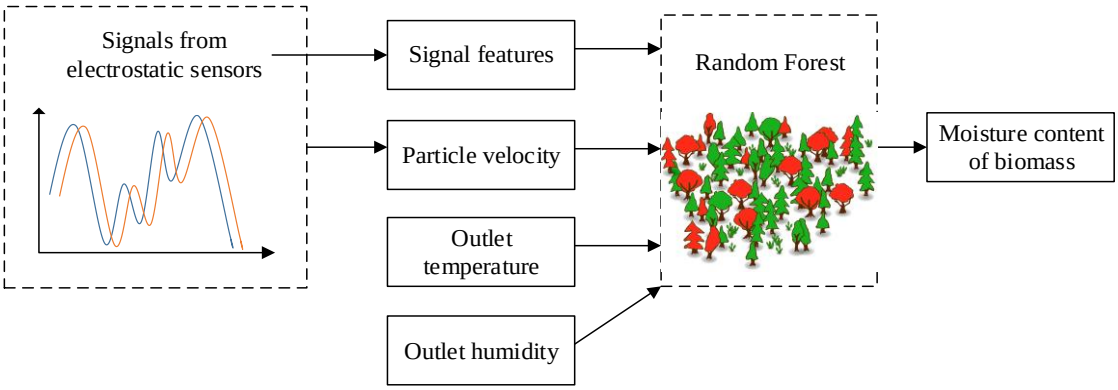

Fig. 15. Overall strategy for predicting moisture content using the RF algorithm [50]. Copyright © 2019, Elsevier

D. On-line Particle Sizing

On-line continuous measurement of particle size distribution is desirable in many industrial processes such as power generation, chemical manufacturing and food processing. For instance, during power generation large coal particles due to insufficient pulverisation may lead to incomplete combustion in the furnace and subsequent operational problems, while overgrinding of fuel is uneconomical for the pulverizing system. At present, particle sizing at coal fired power stations is performed off-line, i.e., fuel samples are taken from the pipe and then analysed in a laboratory through sieving or use of laser diffraction equipment [51], [52]. Such off-line particle size analysis is laborious, inefficient and unsuitable for on-line combustion optimisation when fuel diet changes irregularly. In order to develop an online particle sizing system, a variety of techniques have been proposed over the years, including microwave scattering, laser diffraction, digital imaging, acoustic emission detection and electrostatic sensing [53]. Electrostatic sensors, once fully developed for this application, could have advantages over other sensors in terms of cost-effectiveness, simplicity and maintenance.

As a charged particle of a given size passes through an electrode, a certain amount of electrostatic charge is induced on the electrode and the resulting signal from the electrostatic sensor contains information about the size of the particle. Based on this assumption, preliminary studies have been undertaken to explore if a measurement technique can be established for on-line particle sizing.

Zhang and Yan [54] used a wire-mesh electrode to measure the mass median size of particles. As illustrated in Fig. 16, the electrode is of mesh type and made up of two sets of 0.5 mm diameter copper wires which are arranged mutually perpendicular to each other, and the spacing between adjacent wires is 8 mm. The electrode is fitted on an insulation ring which is mounted on a stainless pipe. Since the exposed electrode only takes up a small cross-sectional area of the pipe, the vast majority of particles go through the free space between the wires of the electrode and hence the electrostatic induction is the main sensing mechanism (Section II. A). A parameter, *R*, termed as particle size indicator, is defined and continuously calculated from

$$R = 10 \log \frac{p_1}{p_2} \tag{14}$$

where p_1 and p_2 are the average powers of two sequences derived from the original sensor signal, respectively, and are given by

$$p_1 = \frac{1}{N_1} \sum_{n=1}^{N_1} V^2(n) \tag{15}$$

$$p_2 = \frac{1}{N_2} \sum_{n=1}^{N_2} V^2(n) \tag{16}$$

where $V(n)$ represents the sensor signal with a total of N samples, N_1 and N_2 the numbers of samples with their amplitudes within and beyond the band ($\bar{V} - 1.7\sigma$, $\bar{V} + 1.7\sigma$), respectively, $\bar{V}$ is the average value of $V(n)$, σ is the standard deviation of the sensor signal, and $N=N_1+N_2$. Through data regression analysis, the relationship between R and the mass median particle size was established. Experimental results obtained on a laboratory test rig indicated that the relative error in the measurement of the particle size was within ±15% under constant mass flow rates. The wire-mesh electrostatic sensor has advantages of high spatial sensitivity and relatively uniform sensing volume. However, as the restrictive nature of the mesh electrode can block the particle flow and will suffer from wear problems, this type of electrode is unsuitable for the on-line particle sizing of pulverised fuel in a pneumatic conveying pipe. For the size measurement of fine dust in ultra-dilute particle laden flow, such as particulates in industrial flues and

chimneys where the flow velocities are much lower than those in pneumatic conveyers, the wire-mesh electrostatic sensor may have a potential to be deployed.

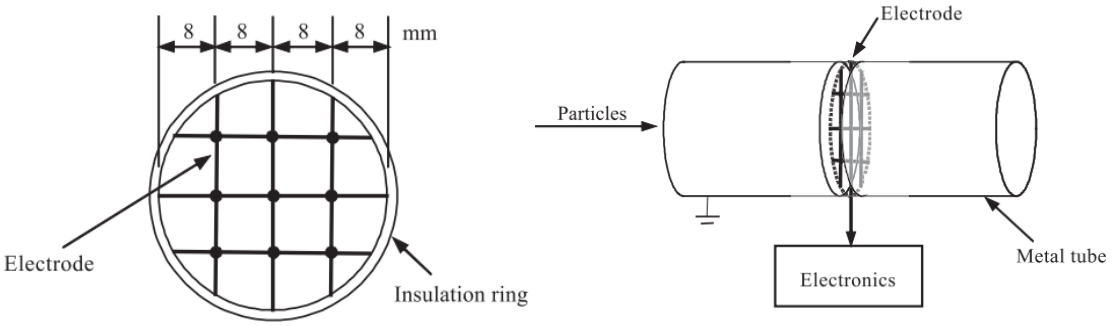

(a) (b)

Fig. 16 Wire-mesh electrostatic sensor for the measurement of mass median size of particles. (a) Electrode. (b) Sensor installation [54]. Copyright © 2003 Elsevier

Ring shaped electrostatic sensors have also been proposed by several research groups for on-line particle size measurement in recent years [1][55]–[58]. The effect of different sized particles on the signal from a ring electrode was initially observed by Yan *et. al* [1]. Chen *et al.* [55] conducted experimental observations and found that smaller particles carry less charges than larger particles and hence lower signal amplitude. Tajdari e*t al.* [56] investigated the size of a single particle using an insulated ring-shaped electrostatic sensor in the frequency domain. In their work, as shown in Fig. 17, a 20 mm wide electrode was fitted outside an insulated 55.6 mm bore pipe, while particles in different sizes flowed through the electrode. The authors claimed that, when the particles moved along the pipe wall, the frequency of the sensor signal was associated with the particle size. Qian *et al.* [57] proposed a method for on-line particle sizing by using an electrostatic sensing head with three exposed ring shaped electrodes. As illustrated in Fig. 18, a pair of 2 mm wide electrodes were implemented to measure the particle velocity through cross-correlation velocimetry (Section II. D) whilst a separate 10 mm wide electrode, which has a larger sensing volume than that of the 2 mm wide electrodes, was used to acquire the signal for particle sizing. Here the particle velocity is measured to compensate its impact on the particle sizing signal as well as an independent measurand. Through experimental tests it was found that the power spectral density and RMS magnitude of the signal increased with particle size. Moreover, when the air velocity remained unchanged, the particle velocity decreased with particle size, so the slip velocity between the air stream and the particles can also be used as an indicator of particle size. Ring shaped electrostatic sensors are better than

the mesh type in the sense that they are nonintrusive to the flow and thus suitable for the size measurement of pneumatically conveyed particles. However, their poor sensitivity to particles in the central area of the pipe is a clear weakness.

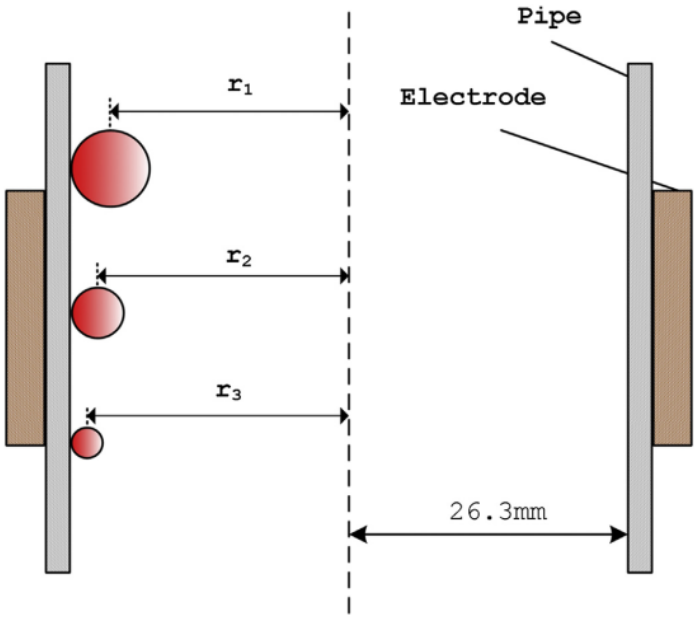

Fig. 17 Particles in different sizes moving along the pipe wall [56]. Copyright © 2014 Elsevier

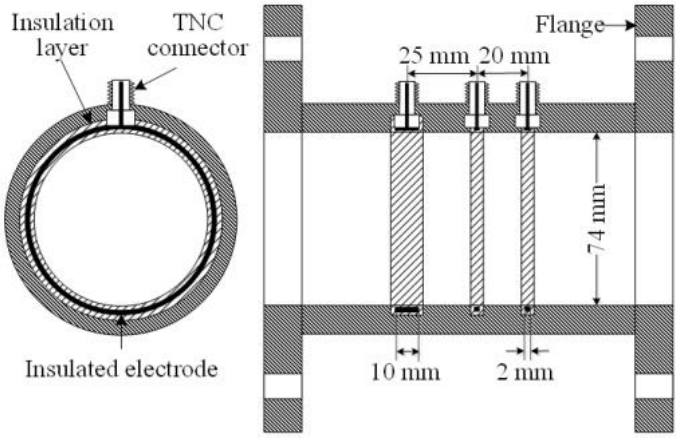

Fig. 18 Electrostatic sensing head with three ring electrodes. [57]. Copyright © 2018, IOP

The electrostatic sensing method presents, in principle, a potential approach to on-line particle size measurement with the aid of a simple electrode and an effective signal processing method. However, despite the earlier attempts, this potential technique is still at a rather rudimentary stage. Significant further work is required to advance the technique, including optimal design of the electrostatic sensor, theoretical studies of the sensing mechanism and establishment of the relationship between the particle size and the characteristics of the sensor signal. It is certainly more challenging to apply the electrostatic sensing technique to measure particle size distribution than average size of particles. Moreover, particle

shape is another factor that should be considered in some applications of on-line particle sizing, for instance, biomass particles in power generation [53].

E. Burner Flame Monitoring

Furnaces are commonly used in many industrial processes to generate heat and power by combusting various fuels such as gas, oil, coal and biomass. In such cases operating conditions should be optimised to maintain high combustion efficiency and low pollution emissions. A burner flame is the central reaction zone of a combustion process. The quantitative measurement of the flame characteristics is thus desirable for an in-depth understanding and subsequent optimisation of fuel conversion and pollutant formation processes.

A variety of flame monitoring techniques [59]–[61] have been developed in order to quantify the characteristics of a burner flame, such as geometric, luminous and thermophysical information. Such techniques are primarily based on the optical, acoustic or thermal emission principles of flames, but electrical properties of a flame have scarcely been utilised for flame monitoring. Moreover, due to the lack of an effective measurement technique for detecting the flame electrical field, little is known about the electrical characteristics of burner flames. Therefore, exploring and developing a novel method for the characterisation of electrical properties of flames is desirable to provide information complementary to that from other techniques and achieve a comprehensive understanding of combustion processes.

It is known that burner flames are electrically conductive because of the existence of positive and negative ions, electrons as well as charged soot particles [62]. Chemi-ionisation reactions in a burner flame, which are sufficiently exothermic to ionise the reaction products, produce a high volume of ions and electrons [63]. The dominant chemi-ionisation reaction in a hydrocarbon flame can be described as [63],

$$CH+O \rightarrow CHO^{+} + e^{-} \tag{17}$$

A significant fraction of soot particles formed in a flame are also charged due to thermal ionisation or diffusive charging [64]. Although the flame is electroneutral as a whole [65], the density and species of ions, electrons and charged soot particles vary in different regions of a flame. Moreover, the spatial

distribution of ions, electrons and charged soot particles vary with time due to the instability of the combustion processes and the complex interaction between gaseous and solid phases. Therefore, information about the combustion process can be obtained by sensing the ions, electrons and charged soot particles in the flame. Preliminary research on electrical properties of a flame [66]–[71] has been conducted to determine its characteristics, including ion density and distribution, flame location and oscillation frequency. Despite the various effort in characterizing the electrical properties of flames over the years, significant issues on the electrical properties of flames remain to be resolved.

For the measurement of ion density and its distribution in a flame, the most common method is measuring the ion current to a negatively biased electrostatic probe that uses the burner as the reference electrode [66], [67]. The electric field applied across the flame induces a body force on the charged species in the same or opposite direction of the field lines, as illustrated in Fig. 19. When the collector and reference electrodes are respectively biased positively and negatively, the negatively charged species (usually free electrons) are attracted to the collector electrode whereas the positive ions to the reference electrode. When the charged species reach the collector electrode, their charge is neutralised, resulting in a net current flow. However, in these studies, the performance of the sensing probe such as the sensitivity have not been fully examined. In order to obtain an in-depth understanding of the mechanism of the reaction that produces ions, it is advantageous to compare the ion-concentration profile with other characteristic profiles in the flame, such as profiles of the temperature and heat-release rate. Langmuir probe was adopted to obtain the profile of positive ion concentration in a lean methane-air flame [68] and it has been found that the maximum ion concentration almost coincides with the maximum of the heat release rate, indicating that the chemi-ionisation reaction in a hydrocarbon flame is closely related to overall reaction rate. Moreover, the ion generation rate has been identified as a promising alternative indicator for the thermoacoustic instability and dynamic response of a combustion process [68].

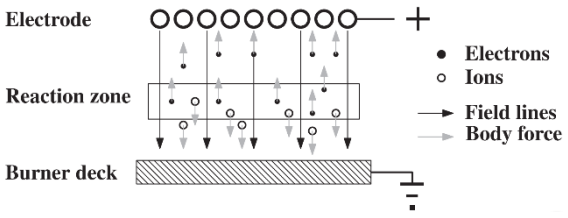

Fig. 19. Schematic representation of the influence of an external applied electric field on the charged species in a flame [67]. Copyright © 2003, Elsevier

A probe, consisting of a platinum wire and a supporting stainless steel tube, is shown in Fig. 17. The supporting tube is used as a reference electrode, which is different from the flame ionised detector. The wire and the supporting tube are connected to the cathode and anode of a DC power supply, respectively, so that the outer tube functions as a reference electrode. The reference electrode is made very close to the detection wire, so they both are immersed into the flame field at almost the same location to suppress noise. Two identical probes were used to estimate the displacement speed of the reaction region in a furnace via cross-correlation of the two ion current signals [69]. The axial length (Ls) of the reference electrode outside the ceramic tube, as shown in Fig. 20, was varied to study its effect on the detection sensitivity. Since the platinum wire senses the ion density and can thus detect the arrival of a flame at the tip section of the probe. Nevertheless, such a probe is a point detection device and the flame movement can only be inferred from a set of probes. It should be pointed out that this type of ion current probe is biased using a DC voltage supply, so the charge can move under the force of the electric field and hence generate a current signal. The design and operation of such an “active” sensor probe are very different from the passive electrostatic sensors which are used in other applications.

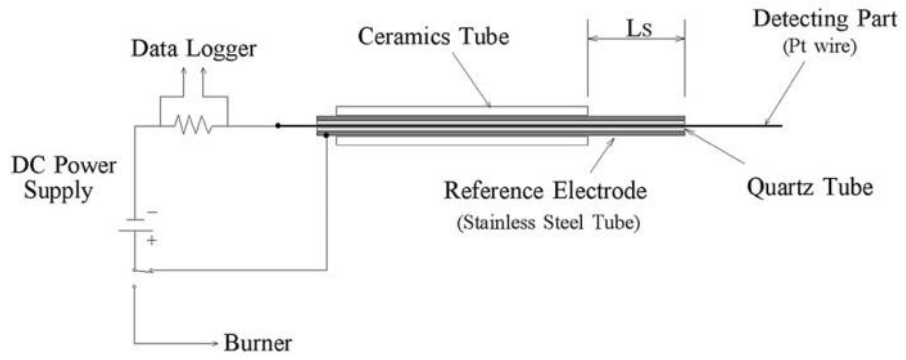

Fig. 20. Schematic diagram of the ion current detection probe [69]. Copyright © 2007, Elsevier

The measurement of the oscillation frequency of a burner flame was achieved through spectral analysis of the ion density signal from an active sensor [70] or the signal from a passive electrostatic sensor [71]. Li *et al.* [70] adopted an ion density probe to acquire the flame signal, as shown in Fig. 21, and determine the oscillation frequency of the flame through spectral analysis. The weighted average frequency of the flame signal was found to be consistent with those from a photodiode flame detector and

a digital camera. However, an external electric field had to be applied to the electrodes, which adversely affects the stability, shape and burning rate of the flame.

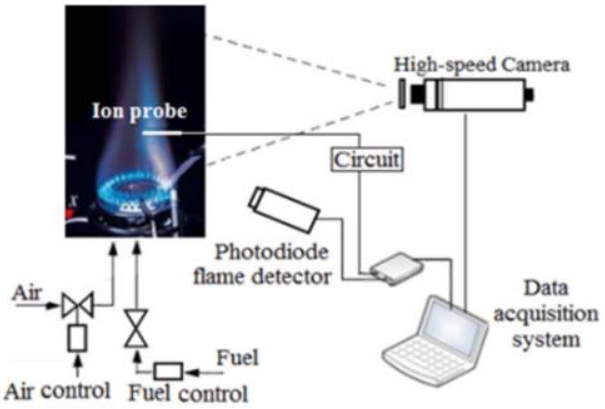

Fig. 21. Measurement of flame oscillation frequency using an ion-current sensor [70]. Copyright © 2015, IEEE

Wu *et al.* [71] developed an electrostatic sensor to measure the oscillation frequency of a burner flame. Fig. 22 illustrates the sensing principle and arrangement of the measurement system. The sensor was placed in the proximity of the flame to detect the amount of transferred charge on the electrode surface. In response to the movement of the flame shape, i.e., the variation in the distance between the electrode and the flame boundary, the exposed electrode generates a current signal. A current-to-voltage converter is used to convert the current signal to a voltage signal and then the information about the variation rate of the flame shape is derived. Power spectral analysis of the signal is performed to obtain their frequency components. The structure and design of the electrostatic sensor are illustrated in Fig. 23. The sensor consists of an exposed electrode made from stainless steel, a quartz insulating strip and a grounded shield. Experimental results were found to be consistent with those from a proven flame imaging system, suggesting that the electrostatic sensor is capable of measuring the oscillation frequency of a burner flame and hence flame stability. More recently, a linear electrostatic sensor array has been used to measure the boundary of a gaseous flame [72]. The results from the sensor array are in close agreement with those from the same flame imaging system.

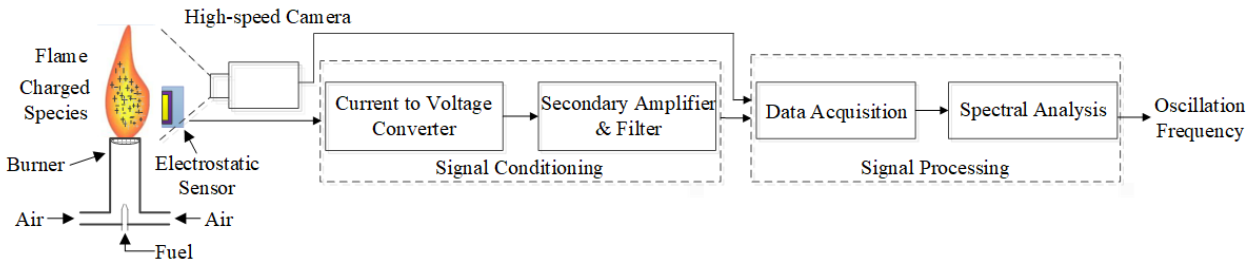

Fig. 22. Sensing principle and arrangement of the measurement system [71]. Copyright © 2018, IOP

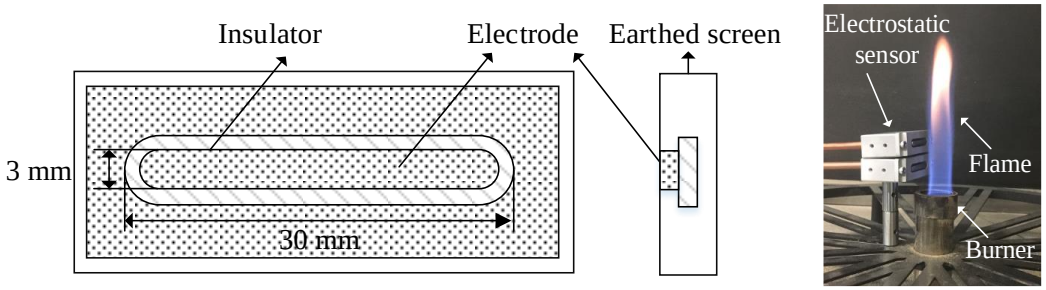

Fig. 23 Electrostatic sensor for the measurement of flame oscillation frequency. (a) Electrostatic sensor. (b) Sensor installation [71]. Copyright © 2018, IOP

F. Speed and Radial Vibration Measurement of Mechanical Systems

Measurements of linear and rotational speeds and vibration parameters (displacement, velocity, acceleration and vibration frequency) are essential for the condition monitoring and control of mechanical machineries in many industrial processes. Even though a variety of speedometers and tachometers based on optical, electrical and magnetic principles are commercially available, there are still disadvantages and limitations that restrict their operability in industrial environments. Therefore, low-cost and non-contact instruments with increased accuracy are desirable.

1) Linear speed measurement

Linear speed measurement of a moving surface such as sheet metal, plastic, textile, rubber and cable are necessary to obtain an accurate and reliable value for strip cutting machines in production and manufacturing processes. When a non-antistatic strip moves in contact with the air and mechanical elements in the system, the surface of the strip is charged due to the friction between the strip and the air and mechanical elements. Yan *et.al.* proposed a speed measurement system based a pair of electrostatic sensors, as shown in Fig. 24 [73]. The speed of the strip is determined from the known fixed spacing between the two electrodes and the time delay between the two signals through correlation. The electrodes used in this research are 40×2 mm wide strips of copper with a centre-to-centre spacing of 20 mm. Through experimental tests it was found that the relative error of the speed measurement system was within ±1.8% with a repeatability of less than 2.5% over the speed range of 0.8 to 10 m/s.

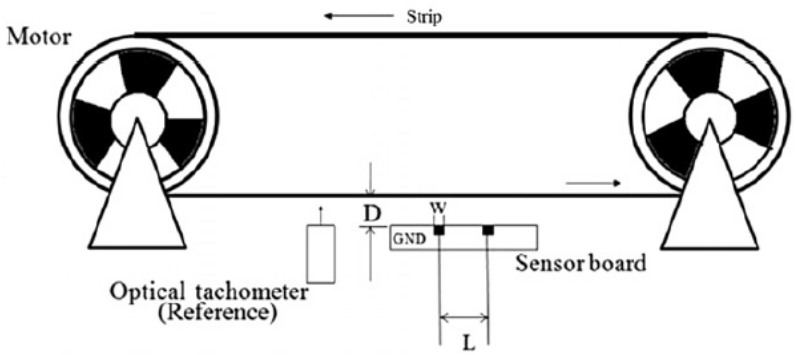

Fig. 24. Test rig for strip speed measurement using electrostatic sensors [73]. Copyright © 2011, IOP

2) Rotational speed measurement

Due to the relative motion between the surface of a non-conducting rotor and the air, electrostatic charge is generated on the rotor surface. Wang and Yan [74] proposed a novel method for rotational speed measurement based on electrostatic sensors and correlation signal processing algorithms. The electrodes used in this case are in a strip shape (Section II.B). In order to optimise the design of the electrodes in terms of geometric dimensions and installation distance to the rotor surface, a mathematical model was developed to investigate the effects of these factors on the characteristics of the sensor, including spatial sensitivity, spatial filtering effect and signal bandwidth [75]. Subsequently, three different configurations based on a single sensor, dual sensors and quadruple sensors, as shown in Fig. 25, were evaluated for rotational speed measurement. The performance of the system in different configurations was assessed on an experimental test rig in terms of measurement range, accuracy, repeatability and stability [13], [74], [76]. The maximum error from the measurement system is within ±2% under all test conditions. Due to the increased number of sensors and effect of multi-sensor data fusion, the quadruple sensor based system has the advantages of faster response, higher accuracy and better robustness. However, the metallic shield required for the installation of the sensors is impractical for a large rotor, whilst the installation of a single sensor or dual sensors based systems are straightforward and flexible. In comparison to a single sensor based system, the dual sensor system has a wider measurement range (including lower speeds) and faster response to speed change.

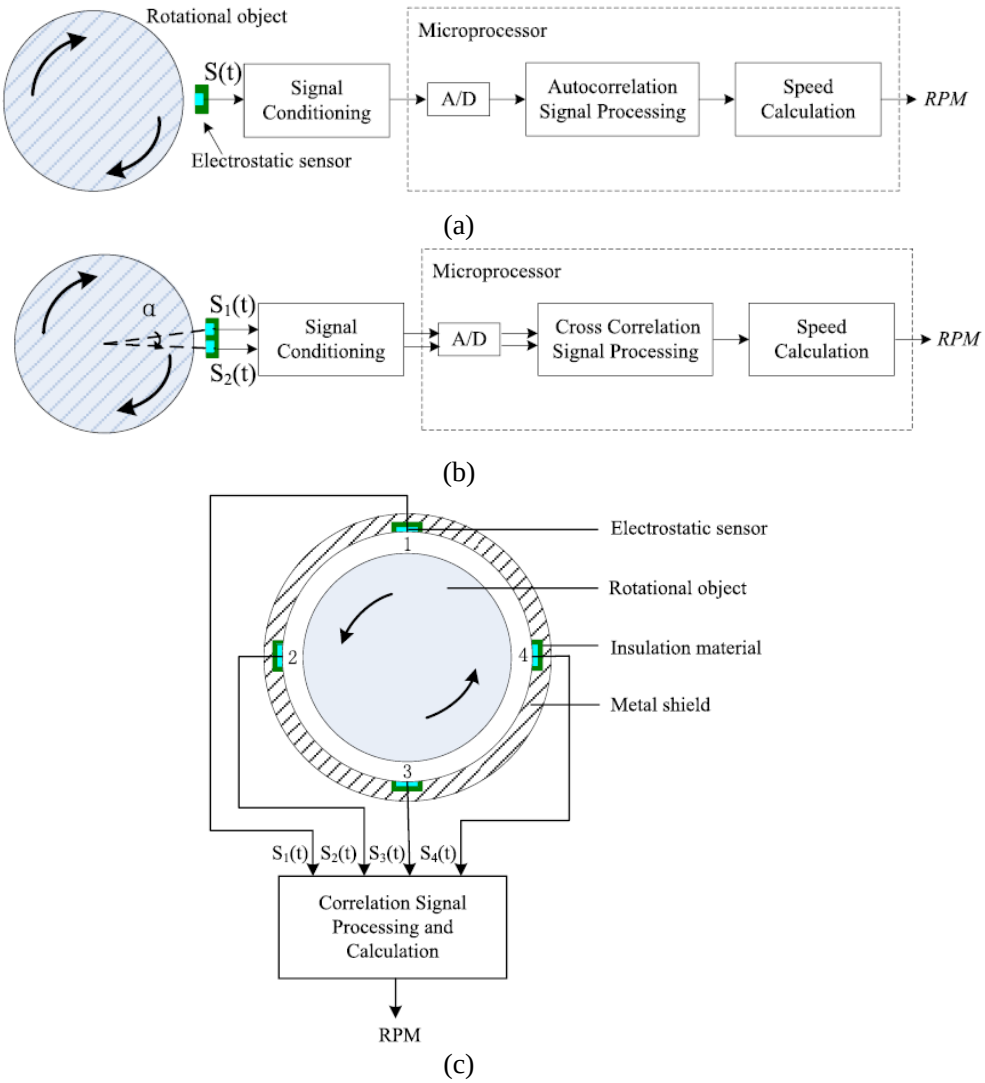

Fig. 25. Rotational speed measurement systems with a different number of electrostatic sensors. (a) Single sensor. (b) Dual sensors. (c) Quadruple sensors [13][74]. Copyright © 2015, 2014, IEEE

The effects of the material and surface roughness of the rotor were studied by finite element modelling and experimental analysis [76]. Meanwhile, different electrode shapes and sensor output characteristics were assessed through mathematical and computational modelling [77]. Research has found that the sensor with a butterfly-shaped electrode slightly outperforms that based on a strip-shaped electrode in terms of spatial sensitivity and frequency response. However, further work is required to optimise the geometric shape of the electrode.

In order to improve the accuracy and robustness of the measurement system based on a single sensor and auto-correlation signal processing techniques, a double autocorrelation method has been proposed [78]. In this method the period of the sensor signal, i.e., the period of the rotational motion, is determined through a double autocorrelation function. The original sensor signal is processed by applying the autocorrelation operation twice in order to inhibit the influence of noise in the signal and smoothen the

waveform around the dominant peak in the correlation function. In consideration of the application of the electrostatic sensing system in a hostile environment such as high temperature and high dust level, Li *et al*. [79] added a comparator hysteresis circuit in the signal conditioning unit to convert the analogue signal from the sensor to a square waveform. It is claimed that the digital approach is capable of eliminating the influence of the sampling rate and noise. However, this conclusion was derived from the results that were obtained from a data acquisition system with the sampling rate of 2 kHz and 5 kHz, respectively. The feasibility of this approach should be further investigated with high-performance hardware. In terms of the dual sensors based system, a data fusion algorithm was proposed by Wang and Yan [80] to improve the measurement accuracy, rangeability and robustness. Based on the two signals form the dual sensors, two independent speed can be obtained through auto-correlation processing of each signal and the third rotational speed by cross-correlating the two signals. Experimental results suggest that the measurement error has been reduced from ±1.5% to ±0.5% by fusing the three independent speed measurements. Since the original signals from electrostatic sensors are susceptible to contamination in a hostile environment, a novel correlation signal processing algorithm was applied by Reda and Yan [81] through a denoising process to minimise the impact of noise in the signal and improve the performance of correlation-based speed measurement. The improved system is mostly within ±0.1% over the speed range of 300-3000 rpm and within ±0.2% over the speed range of 40-300 rpm.

3) Vibration measurement

For the detection of rotor vibrations a range of techniques are available to measure the displacement, acceleration and vibration frequency of a rotor [82], [83]. Through the analysis of signals from electrostatic sensors, Wang and Yan [84] have found the signals contain useful information about the overall operating conditions of the rotating machinery. By using signal processing algorithms, including signal amplitude analysis and Hilbert-Huang transform, vibration direction and frequency are extracted from the signals [84], [85]. It must be made clear that aforementioned electrostatic sensors can be used to measure the rotational speed and vibration of non-conducting rotors. For metallic rotors, however, dielectric or electret markers required to be placed on the rotor surface to generate charge pattern for

measurement. As shown in Fig. 26, eight charged markers made of 2×2 mm^2 electret film (a quasi-permanently charged material) are fixed along the circumference of the shaft. As the amplitude of the signals is affected by the ambient temperature and humidity, Reda and Yan [86] employed the frequency response properties of an electrostatic sensor to detect and quantify the displacement of an unbalanced shaft. The electrostatic sensor and signal conditioning circuit are shown in Fig. 27.

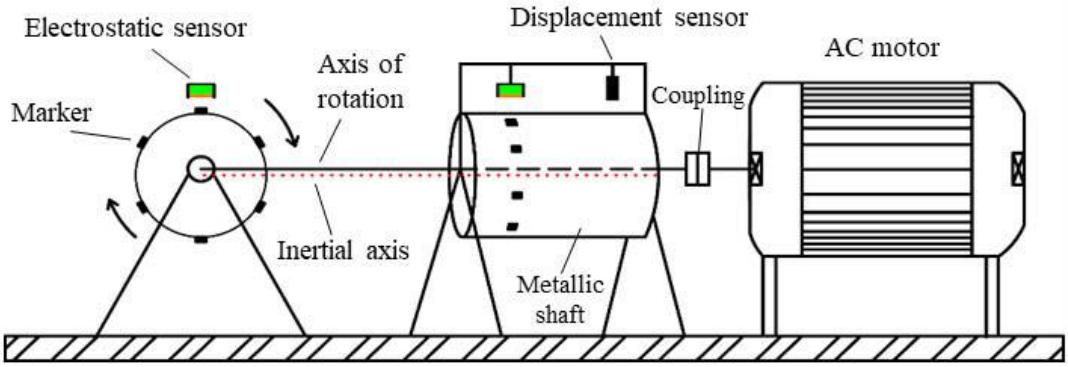

Fig. 26. Vibration measurement system [86]. Copyright © 2019, IEEE

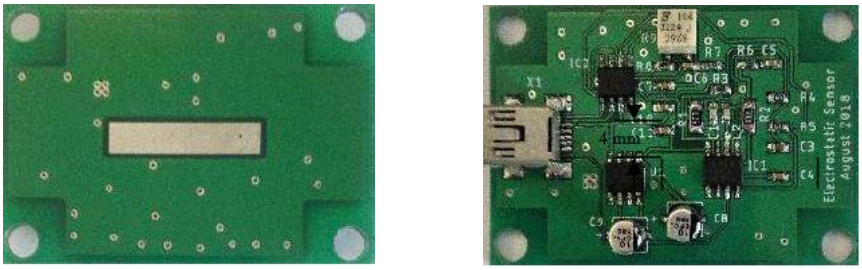

(a) (b)

Fig. 27. Electrostatic sensor and signal conditioning circuit. (a) Electrode layer. (b) Components layer [86]. Copyright © 2019, IEEE

Experimental tests were undertaken on an eccentric metallic shaft with a diameter of 60 mm and eccentricity of 0.5 mm from the rotation axis. Results have shown that the system is capable of providing displacement measurement with a maximum error of ±0.6% [86].

G. Condition Monitoring of Power Transmission Belts

Power transmission belts are widely used to transfer torque between pulleys in many industries, in particular, manufacturing, automotive, agricultural and power generation sectors. Usually, the belt axial velocity is determined from the rotational speed of the pulley, which is easy to measure using a range of sensors. However, the slippage between the belt and the pulley can lead to significant errors when determining the belt axial velocity. The compliance of the belt material and various mechanical defects may result in abnormal belt vibration and hence performance degradation and even failure of a machine.

On-line measurement of the axial velocity and transverse vibration of power transmission belts facilitates the detection of incipient faults and predictive maintenance. There exist several techniques for the condition monitoring of power transmission belts, including digital imaging and laser Doppler vibrometers [87], [88]. However, these techniques are complex, expensive and unsuitable for routine applications in harsh industrial environments.

A non-conducting belt, usually made of rubber, fabric or thermoplastic material, can be electrified because of physical contact and friction with the pulleys. Consequently, a fluctuating electric field is generated around the belt which undergoes combined axial and transverse motion. The variation of the electrostatic field permits the measurement of belt kinematic parameters using electrostatic sensors. Hu *et al*. [10], [89]–[91] conducted a systematic study of the measurement of axial velocity, transverse vibration and operating deflection shapes (ODSs) of a power transmission belt using the electrostatic sensing technique. The fundamental problem in this research is to establish how the electrostatic sensor responds to the motion of the belt. The method of moments [10] was used to calculate the level of induced charge on the electrode under different conditions in order to elucidate the sensing mechanism. The belt was modelled as a chain of point charges that follows a travelling wave trajectory, which represents the simplified belt motion, as shown in Fig. 28. The calculated induced charge on two strip-shaped electrodes placed in parallel with the axial direction of the belt shows that two sinusoidal charge signals with the same waveform but a time delay between them are produced. The fluctuation of the induced charge arises from the variation of the distance between the belt and the electrode, while the time delay steps from the propagation of the travelling wave from the upstream to the downstream electrodes.

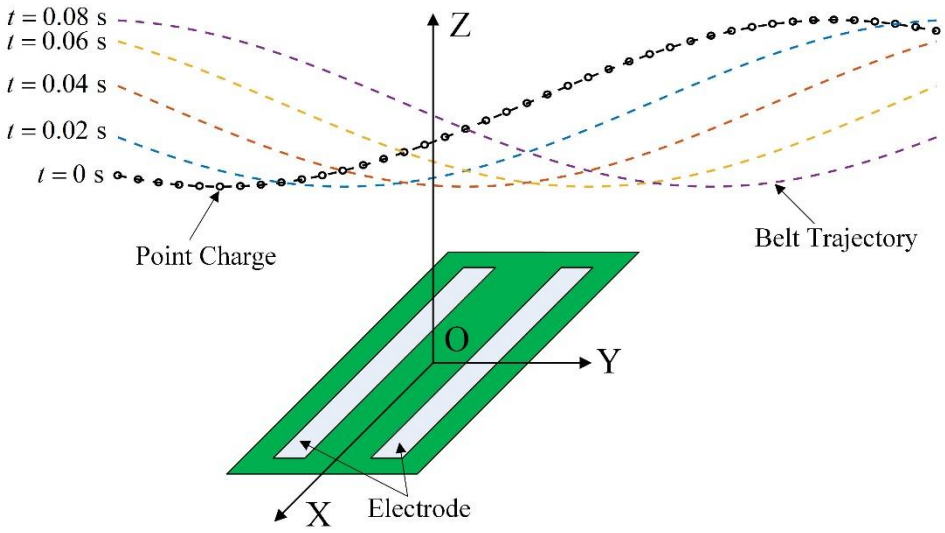

Fig. 28. Simulation of the sensor response to belt motion [10]. Copyright © 2017, IEEE

The simulation results suggest the feasibility of measuring belt axial velocity using electrostatic sensors. In [10], [89], the transit time taken for the belt to pass the two electrodes was determined by cross-correlating the two signals from the electrostatic sensors. With the known distance between the electrodes, the belt velocity was calculated directly by dividing the distance by the transit time. The accuracy and reliability of the measurement system were improved by fusing measurement results from multiple pairs of sensors with the correlation coefficients used as the weights [89]. Experimental results have shown that the belt velocity can be measured with a relative error within ±2% from 2 to 10 m/s.

Measurement of the transverse belt vibration has been attempted by analyzing the spectra of the sensor signals. Two types of signal conditioning circuits, namely charge amplifiers and transimpedance amplifiers [10], [90], are developed to convert the induced charge and current into voltage signals, respectively. The induced charge signal, which depends on the distance between the belt and the electrode, represents displacement measurement, whereas the induced current signal, as a time derivative of the induced charge signal, represents velocity measurement. Displacement and velocity spectra of the belt transverse vibration are thus obtained. Although the vibration modes can be correctly identified from both spectra, the magnitude of the transverse displacement and velocity cannot be determined because of the vulnerability of the triboelectric charge on the belt to environmental and operating conditions. In addition,

since the spatial sensitivity of the sensor is non-uniform, higher order harmonics are introduced to the vibration spectra [90].

Based on the vibration measurement results the belt ODS was measured using a linear array of electrostatic sensors placed along the length of the belt, as shown in Fig. 29 [91]. By selecting a fixed reference sensor, ODS frequency response functions (FRFs) which include the vibration magnitude and the phase shift were calculated for all sensors. An ODS vector was constructed from the imaginary components of the FRFs at the vibration frequency. Fig. 30 shows the measured ODSs at a belt axial velocity of 4 m/s. As illustrated, similar deformation patterns are exhibited by the ODSs at the first three vibration frequencies, while the amplitudes differ considerably.

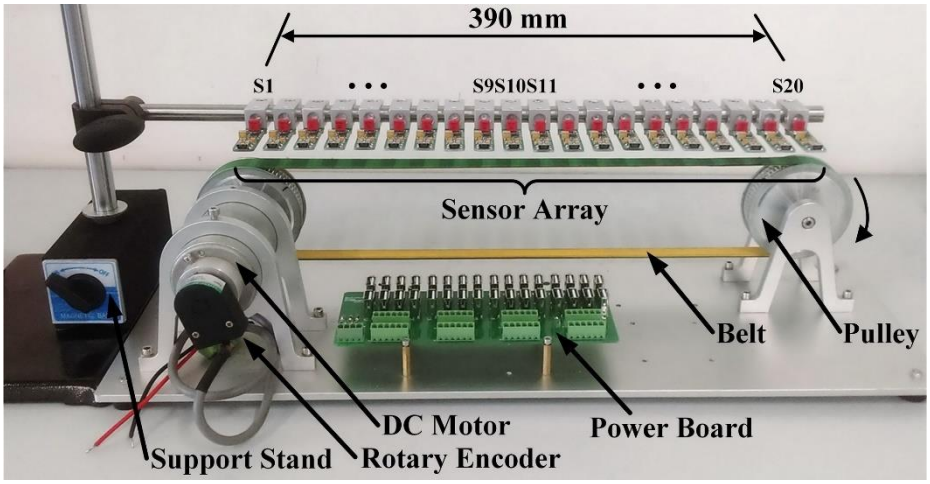

Fig. 29. Measurement of ODS using an electrostatic sensor array [91]. Copyright © 2017, IEEE

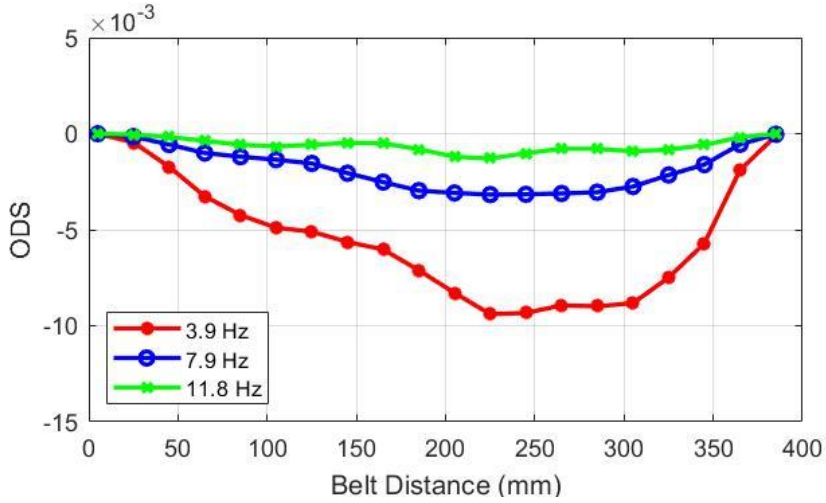

Fig. 30. Measured ODSs when the belt axial velocity is around 4 m/s [91]. Copyright © 2017, IEEE

The combined axial and transverse motion of power transmission belts preclude the applicability of most existing speed and vibration measurement systems. In comparison to existing digital imaging and

laser Doppler techniques, electrostatic sensors have the advantages of simplicity in structure, cost-effectiveness, easy installation and applicability to various environments. It is envisaged that his technique will be deployed to monitor belt conditions in many industries in the near future.

H. Condition Monitoring of Mechanical Wear

Condition monitoring of mechanical wear is essential to assess the health status of mechanical components and systems. Compared to conventional techniques based on vibration monitoring and temperature detection for condition monitoring of mechanical wear and associated prognostics, the electrostatic sensing technique offers a better or complementary means to provide timely warning of developing faults [92]. In this case electrostatic sensors detect charged debris resulting from the wear of mechanical parts or systems. In recent years, significant research has been undertaken to explore the applications of electrostatic sensors for the condition monitoring of aero-engines and bearing wear.

1) Condition monitoring of aero-engines

Aero-engines are very complex but safety critical systems. To ensure the operational safety and reduce downtime of aero-engines, prognostic and heath management systems are highly desirable. There exist a range of charged particles such as ions, electrons and soot in the exhaust section of the combustion process. In principle, the condition monitoring of an aero-engine can be realised using electrostatic sensors to detect the overall level of electrostatic charge in the exhaust gas path of the aero-engine. Under healthy working conditions the level of charged particles in the exhaust emission path of an aero-engine remains within a normal range. Even though the charge level naturally fluctuates with operational conditions of the engine, such a variation would be relatively smooth and repeatable with the same transition. However, a sudden increase in the charge level stems from the presence of debris due to the significant mechanical wear of the system such as blade rubs, nozzle guide vane or turbine blade erosion and combustor burning. Electrostatic sensors are usually fitted in the inlet and exhaust pipe sections of an engine to detect ingested and exhaust debris.

Powrie and Worsfold [93] investigated the use of an Engine Debris Monitoring System (EDMS) for the monitoring of gas path component deterioration in a heavy-dusty gas turbine. The electrostatic sensor, as shown in Fig. 31 was mounted in the exhaust duct of the gas turbine.

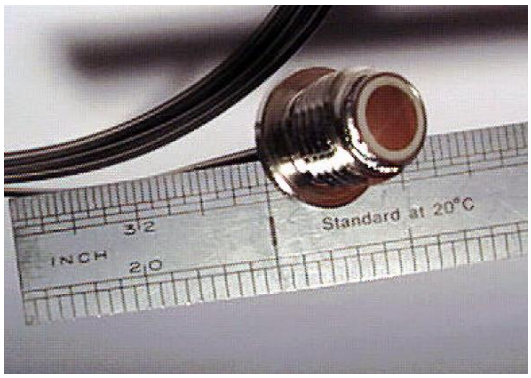

Fig. 31. Electrostatic sensor used in EDMS [93]. Copyright © 2001 by Powrie *et. al.*

The charge signal from the sensor is converted into a voltage signal through a signal conditioning unit. The EDMS was applied to monitor the condition of the gas turbine at Connah's Quay Power Station over seven months under different operational conditions, including run-ups, shutdowns and variable load conditions. The activity level was observed and studied, which is a measure of the high frequency content of the sensor signal and relates to the amount of fine particulates in the exhaust gas. Meanwhile, shaft order analysis was performed under different conditions to establish whether the production of the gas path debris correlates with the shaft speed as well as the likely faults of rotating components.

Novis and Powrie developed an engine Ingested and Exhaust Debris Monitoring System (I/EDMS) [94], [95]. As shown in Fig. 32, the sensing element used at the ingested part of the combustion system consists of two ring shaped electrodes on the inner surface of the inlet duct while a single-button sensor was mounted in the exhaust duct of the engine. The IDMS was used to detect debris in the gas path due to component faults, in addition to discrete foreign objects such as pebbles, washers, lock-wire etc. The system was also sensitive to particulates or fluid ingestion such as sand or salt-water. However, the reports [94], [95] focus mainly on the hardware design of the system, giving very little technical details of the signal processing elements with no detailed explanation of the purpose of using two identical ring electrodes in the sensing unit.

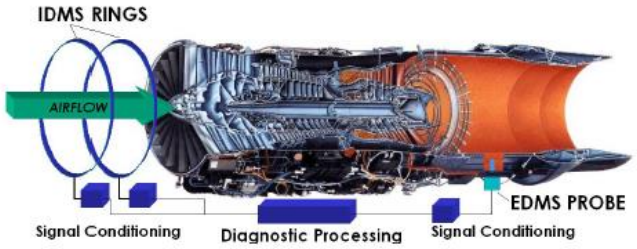

Fig. 32. Ingested and exhaust debris monitoring system [94]. Copyright © 2006, IEEE

Wen *et al*. [96] presented the electrostatic sensing technique for the condition monitoring of aero-engines, focusing sensor design, de-nosing methods, feature extraction and fault identification algorithms. Nickel alloy and ceramic were used as the electrodes and isolation material, respectively, to enhance the mechanical strength and durability of the sensor. A combination of empirical mode decomposition and independent component analysis was deployed to remove the noise in the sensor signals. Apart from the statistical parameters (e.g. maximum value, minimum value and RMS), three features including activity level, event rate and energy distribution were quantified from the signals to differentiate normal and abnormal particles detected. The activity level (L_a) is an indicator of the amount of fine particulates in the exhaust gas such as smoke, soot or other small debris. L_a is defined as:

$$L_a = \sqrt{\frac{1}{N}\sum_{n=1}^{N} Q_n^2} \tag{18}$$

where N is the number of samples of the induced charge signal (Q) in each measurement cycle. L_a is, in fact, the RMS magnitude of the charge signal.

Event rate (R_e) relates to the number of larger particles (approximately 40 microns or greater) present in the exhaust gas per unit time. R_e is defined as

$$R_e(t) = \frac{M}{N} \times 100\% \tag{19}$$

where M is the number of samples of the induced charge (Q), which meet $|Q_n| > K \times AL$, where K is a constant determined through experimentation. Note that R_e can be positive or negative, depending on the polarity of the charge signal.

Energy distribution is obtained by calculating the energy density of the signal in different frequency bands. Experimental tests were conducted to generate continuous small carbon particles, discrete large

carbon particles and discrete large metal particles, respectively. Results have shown that L_a and R_e increased significantly due to the injected particles. The polarity of R_e can discriminate carbon particles (positive R_e) and metal particles (negative R_e). Moreover, the abnormal particles (metal particles) result in increased energy distribution in the low frequency band. Based on the experimental data obtained under different conditions, a rule based fault recognition algorithm was developed to identify normal status, combustion efficiency degradation and rub fault.

With the electrostatic monitoring system developed in [96], a series of experimental tests was conducted on turbojet engines and civil turbofan engines [97]–[100]. To optimise the design of the sensors, finite element models of rod-shaped electrodes with different structural parameters were developed by Wen *et al.* [101]. The sensitivity and frequency response of the models were analysed. The results have shown that the radius of the rod has little effect on the sensitive space of the electrode. The sensitivity of the sensor increases with the higher permittivity and thinner layer of the isolation medium. In addition, the signal induced by fast-moving and continuous particles has a broader frequency bandwidth and more high frequency contents. As the rod-shaped electrode is restrictive to the gas flow, Chen *et al.* [102]–[104] proposed circular thin-plate and hemisphere-shape electrodes. The performance of these sensors was evaluated through mathematical modelling and simple validation experiments. However, the performance of the sensors in monitoring aero-engine gas path is still unknown. Through physical modelling, Addabbo *et al.* [105] derived the analytical expression of the time-varying charge induced by the moving debris on the sensor surface and discussed the effect of the amplifier bandwidth on the shape of the signal. Most recently, the same team proposed theoretical methods to estimate the trajectory and velocity of a moving charged particle based on an array of circular electrostatic sensors [106]. Fig. 33 illustrates the mathematical model of the electrostatic sensor array. The proposed methodology was assessed through numerical simulation and experiments conducted on an experimental physics emulator. The simulation results suggested that the measurement of the trajectory and velocity has high accuracy and the accuracy of velocity measurement is not affected by the particle trajectory direction. However, there are no experimental results to support the conclusion.

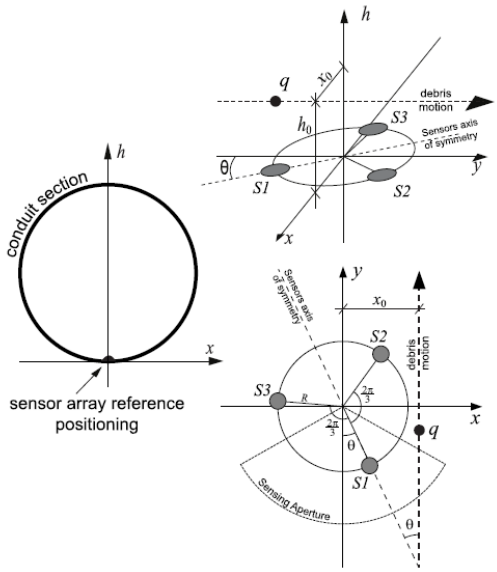

Fig. 33. Mathematical model of an electrostatic sensor array with three-button electrodes [106]. Copyright © 2019, IEEE

2) Condition monitoring of bearing wear

Current on-line condition monitoring of bearings and gears relies on the notable increase in noise and vibration. Electrostatic monitoring of any debris generated by tribo-contacts can provide early warning of component deterioration or failure. Condition monitoring of bearing wear can be achieved by directly monitoring the wear site or detecting the wear debris in lubrication oil. Tasbaz *et al*. [107] investigated the possibility of detecting scuffing at the point of contact using electrostatic sensors. Experimental tests were conducted on a pin-on-disc wear rig and a plint TE/77 high frequency wear rig. As shown in Fig. 34, the primary sensor with a ring-shaped electrode was used to detect charge generation at or near the point of contact. The secondary sensor in a button type (Fig. 34(a)) and the line type sensor (Fig. 34(b)) were used to monitor charge transportation away from the contact site. The oil was fed to the contact point before starting experimental tests so that the electrostatic charge would be generated from the friction between the steel ball, the oil and the plate. Results have shown that slight mechanical wear can be detected from the signals acquired from the primary electrostatic sensors prior to severe scuffing. Moreover, the charge generated at the contact area exists long enough to be detected by a secondary sensor which is relatively far from the contact point. It is possible to detect charge transportation within the oil or on a metallic surface.

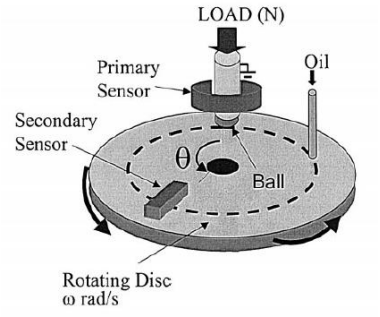

(a)

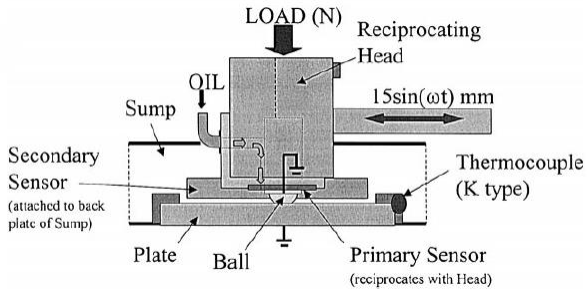

(b)

Fig. 34. Test rigs for electrostatic monitoring of oil lubricated sliding point contacts. (a) Pin-on disc wear rig. (b) Plint TE/77 high-frequency wear rig [107]. Copyright © 1999, Elsevier

Harvey *et al*. [108] conducted an experimental investigation into the charging effects of lubricating oil (quality, viscosity, temperature, aging etc.) and the roughness of the disc surface. Further studies of the oil composition on the charging nature were conducted on an oil droplet rig with a range of base and formulated oils [109]. In order to monitor the unlubricated sliding wear of a bearing steel, Morris *el al*. [110] carried out experimental work on a modified pin-on-disc wear test rig. Fig. 35 shows the modified test rig to produce sliding wear in the mild oxidational wear regime. The button type electrostatic sensor was placed approximately 0.5 mm above the disc surface. The results have demonstrated that there is a direct correlation between both the wear rate and coefficient of friction with the magnitude of charge detected.

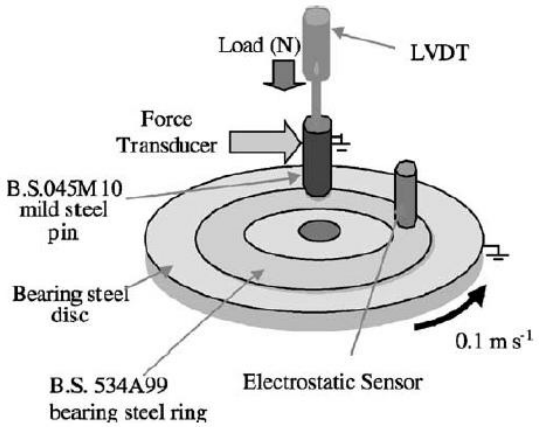

Fig. 35. Test rig for unlubricated sliding wear experiments [110]. Copyright © 2003, Elsevier

Sun *et al*. [111] combined electrostatic sensing and Acoustic Emission (AE) techniques to monitor the various phases of delamination wear. Experimental tests were conducted on a pin-on-disc tribometer (Fig. 36). A button type electrostatic sensor was located 0.5 mm above the disc surface to monitor the charge level on the wear track. An AE wideband transducer was positioned on the top of the pin holder to monitor the AE signals from the contact. Results have shown that three wear regimes, including running-in, delamination and oxidation, can be distinguished through analyzing electrostatic and acoustic signals.

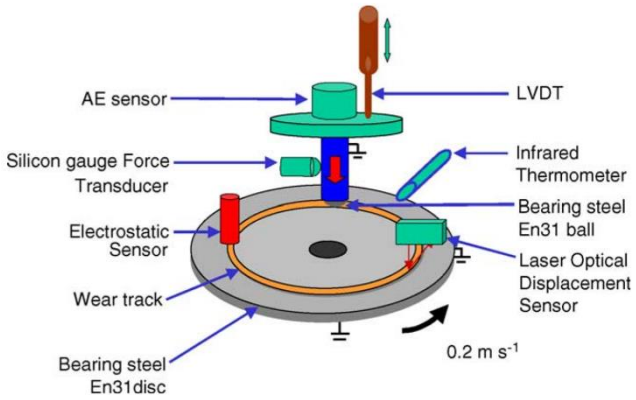

Fig. 36. Pin-on-disc tribometer test rig [111]. Copyright © 2005, Elsevier

A further experimental study was conducted on a taper-roller bearing test rig to assess the performance of a proposed electrostatic monitoring system [112], [113]. The taper-roller bearing test rig is shown in Fig. 37. Two types of electrostatic sensor were used in this research. Three button-type electrostatic sensors were installed in the vicinity of support bearings and test bearings. Two identical ring-shaped electrostatic sensors were situated in the oil recirculation system to monitor charge associated with debris generated during testing. Experimental results have shown that the electrostatic monitoring system detected bearing deterioration up to four hours prior to complete failure. The electrostatic wear-site and oil-line sensors detected changes in charge level which coincided with increases in temperature, vibration and debris generation.

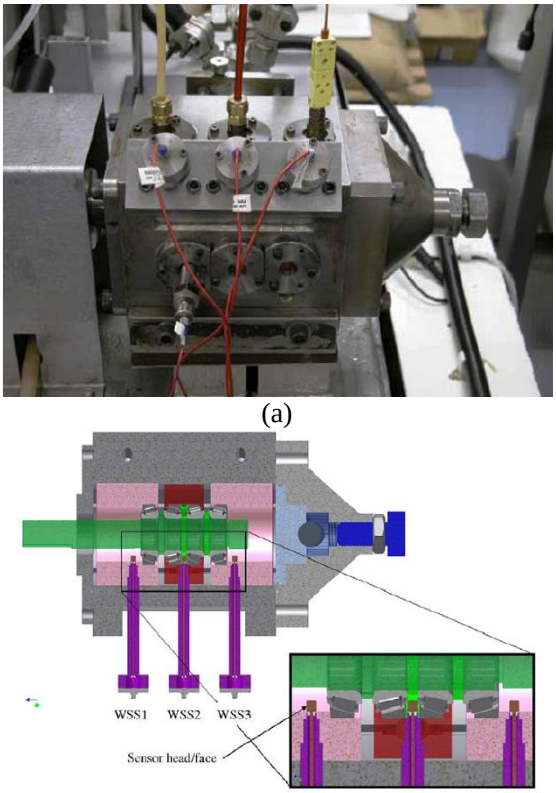

(a)

(b)

Fig. 37. Taper-roller bearing test rig. (a) Photo of the taper-roller bearing test rig. (b) Schematic of wear-site sensors arrangement [112]. Copyright © 2007, Elsevier

To optimise the design of the electrostatic sensors for oil lubricated tribological systems, Liu *et al*. [114] developed mathematical models of the ring-shaped electrostatic sensor and investigated its sensing characteristics, including spatial sensitivity, sensor efficiency, static sensitivity and electrostatic field of view. Through analyzing the possible charge sources in the lubrication system, Mao *et al*. [115] proposed two debris recognition methods based on the amplitude and pulse width of the sensor signal and general extreme value distribution. However, the methods only work when the gearbox is in a stable working condition. The electrostatic sensing system was tested for the monitoring of wind turbine gearboxes [116]. The sensing system consists of two ring electrodes with a spacing of 100 mm which were mounted in the oil recirculation system of the main test gearbox. It is proven that the electrostatic sensor can be used to detect the debris in the oil system by analyzing the peak and pulse width of the signals. The relationship between the number of debris and pulse width was also studied.

I. Human Activity Monitoring

A human body can be triboelectrically charged when walking on an insulating floor or touching a dielectric material such as clothes and various objects in our daily lives [117]. High electric potential

develops as the charges build up on the body. The capacitance between the human body and the ground changes during body movements, mostly due to variations in the distance between the body limbs and the floor [118]. A periodic variation of body electric potential is thus generated as a result of the changing capacitive coupling. The variations in the electric field around the human body allow non-contact monitoring of human activity using electrostatic sensors. This idea has spawned a variety of applications ranging from medical diagnosis and healthcare monitoring, indoor presence detection and localisation, motion sensing, to human-computer interaction. It should be noted that there exist other mechanisms that cause changes in the electric field around the human body, such as biopotential signals arising from the activities of the heart, brain and muscle termed as ECG, EEG and EMG, respectively [119] and perturbation of the electric fields generated by ambient sources such as power lines and appliances due to the presence of a moving human body [120], [121]. However, only monitoring of human activity based on the mechanism of triboelectrification is included here in order to maintain consistency with the main theme of this review. Another point to note is that different terms such as *electric potential sensors* and *capacitive sensors* instead of electrostatic sensors have been used to describe the same technique in the literature.

The respiration activity increases and decreases the distance between the human chest and the electrode, changing the coupling capacitance periodically. Harland *et al*. [122] measured the respiration rate using two electric potential sensors configured as a differential pair at a distance of 2 cm from the chest. Tang and Mandal [121] acquired respiration signals using an Electric Potential Integrated Circuit (EPIC) sensor, which is a commercial version of the electric potential sensor developed by Prance *et al*. [123], [124], with the participant sitting 0.5 m away from the electrode. Kurita [125] presented a theoretical model to analyse the induced current generated by human respiration with an abdomen-electrode spacing of 30 mm. As illustrated in Fig. 38, a transimpedance amplifier was used to convert the induced current at sub-picoampere level into a voltage signal.

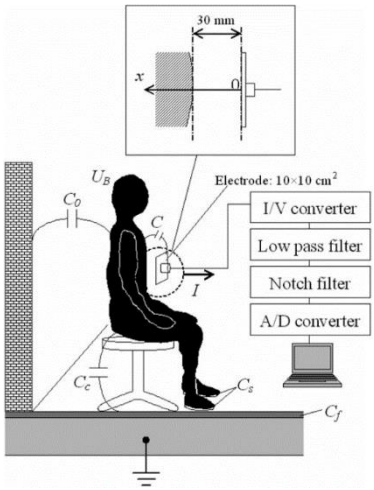

Fig. 38. Detection of human respiration by measuring the electrostatic induction current [125]. Copyright © 2018, Springer Nature

Hand gesture detection and recognition via electric field sensing for human-computer interaction (HCI) has also been proven feasible by a few studies. Kim and Moon [126] used four EPIC sensors located at the screen corners of a smart TV to detect the electric disturbance caused by moving hands and achieved a correct gesture classification rate of 92% at a standoff distance of 1 m. Kurita [127] detected the hand movements via the induced current on four electrodes placed in a square configuration at a distance of 30 cm to the hand. Tang *et al*. [128] determined the three-dimensional position of a hand in real time using an array of five spherical electrodes and a constraint scanning positioning method. Fig. 39 illustrates the experimental setup of hand positioning using electrostatic sensors.

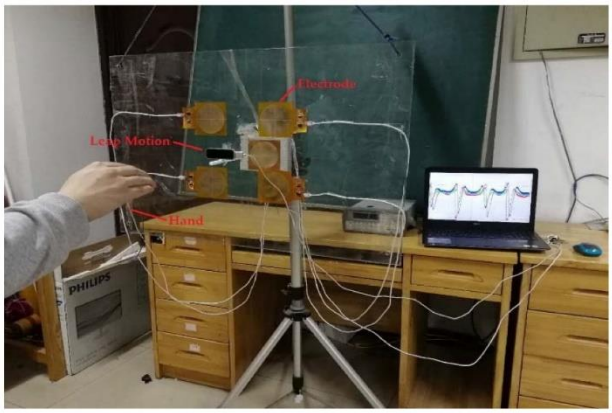

Fig. 39. Experimental setup of hand positioning using electrostatic sensors [128]. Copyright © 2018 by K. Tang, *et. al.*

Based on the same sensing mechanism, walking motion and other leg movements have also been detected and characterised, with potential application for physical rehabilitation, clinical assessment, surveillance and human recognition. The body electric potential during walking was measured by Takiguchi *et al*. [129] using an electrode of 7 m long positioned 1 m above the ground and 50 cm away

from the centre of the walking path. From the recorded waveforms of electric potential, the number of steps was accurately determined for both adults and infants. Li *et al*. [130] measured the temporal gait parameters of walking using the induced current on an electrode located 3 m away from the human. Kurita and Morinaga [131] achieved person identification using the current signal induced by walking. They have also achieved detection of standing up from and sitting down on a chair using an electrostatic sensor, as illustrated in Fig. 40 [132]. Pouryazdan *et al.* [133] detected the leg lifting and shaking movements of a seated person using a wrist-worn electric potential sensor. Similarly, the capacitive coupling between the human body and the environment was measured by Cohn *et al.* [134] to sense the body motion using a capacitive sensor attached to the wrist.

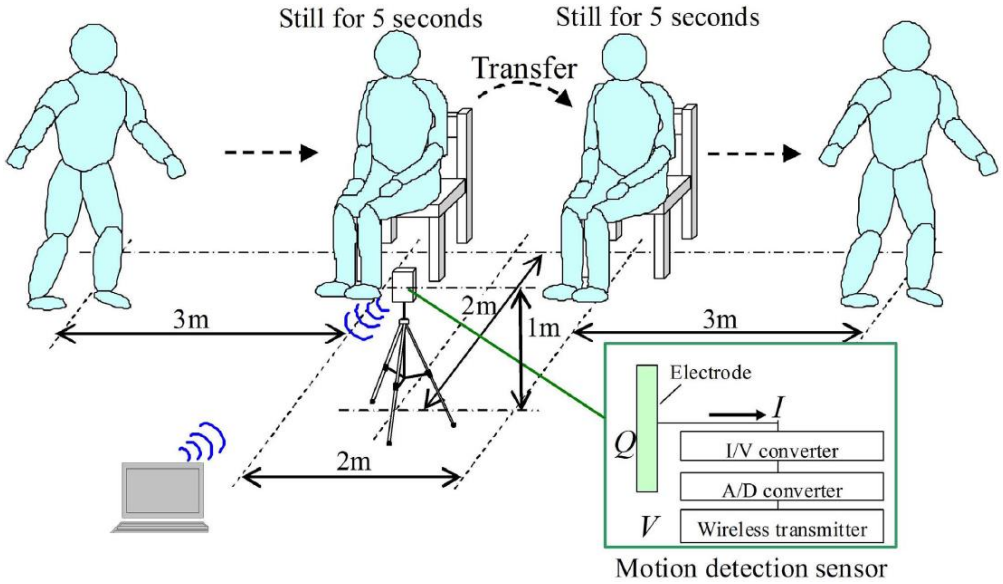

Fig. 40. Daily motion measurement using an electrostatic sensor [132]. Copyright © 2019, IEEE

The sensing of whole body movements can provide information for indoor localisation, which plays an essential role in smart buildings. Fu *et al.* [135] performed indoor localisation by measuring the potential change on wire electrodes arranged in a grid structure under the floor carpet, as illustrated in Fig. 41. The mean positioning error achieved was only 12.7 cm, because of the small wire spacing of 20 cm. In comparison with other indoor localisation methods, the passive electric field sensing method is easy to install, intrinsically safe, unobtrusive, power efficient and cost effective.

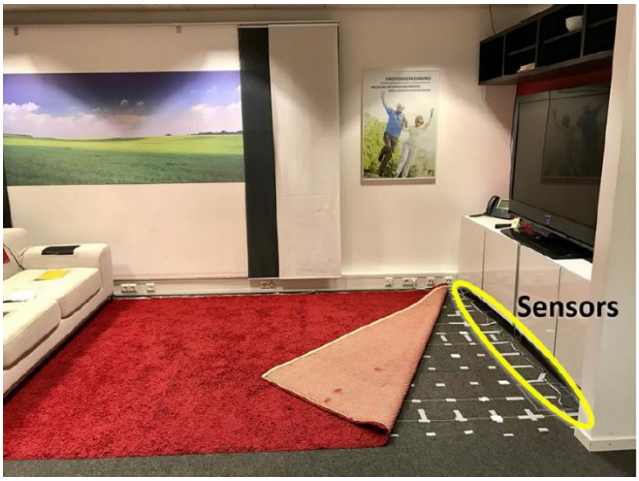

Fig. 41. Indoor localisation using wire electrodes of grid structure [135]. Copyright © 2018, Springer Nature

IV. STATE-OF-THE-ART AND FUTURE DEVELOPMENT

A. State-of-the-Art

The electrostatic sensing technique has emerged as a widespread and attractive means for the measurement or monitoring of a diverse range of processes or systems. Electrostatic sensors provide useful information about a target system or process without mechanically intruding the target being monitored. Table 1 summarises the industrial applications and compares the electrodes and signal processing algorithms or methods used along with the key variables determined from the sensor signals. We have also assigned a Technology Readiness Level (TRL) for each of the described applications in accordance with the definition of TRL [136], based on the current state of its development. In view of the common characteristics of the targets to be measured and monitored, the applications can be broadly grouped in three main areas: (1) multiphase flow measurement and characterisation (flow measurement of pneumatically conveyed solids, measurement of particulate emissions, monitoring of fluidised beds, on-line particle sizing, and burner flame monitoring), (2) condition monitoring of mechanical systems and processes (speed and radial vibration measurement of mechanical systems and condition monitoring of power transmission belts and mechanical wear), and (3) human activity monitoring. All types of electrodes, as outlined in Section II.B, have been proposed and optimised in the applications, so have the signal processing methods (Section II.C). The key variables that have been determined from the sensor signals are wide-ranging, depending significantly on the purpose of the monitoring and measurement for

a given application. The TRL varies also widely from TRL1 - Basic principles observed to TRL9 – Actual system proven in operational environment. Following many years of developments, instruments and devices based on electrostatic sensors for the flow measurement of pneumatically conveyed solids have reached the highest TRL because commercial products have been on the markets for some years and many are in routine operation on coal fired power stations. However, absolute measurement of mass concentration of pneumatically conveyed solids (TRL7) still requires further development. The monitoring of particulate density in industrial stacks has also reached a high maturity (TRL9), though the velocity measurement of particulates and hence mass emissions are around TRL6. Some proposed applications of electrostatic sensors such as on-line particle sizing and burner flame monitoring are still in their earlier stage of development. There is slight uncertainty in deciding the TRL for condition monitoring of mechanical wear and human activity monitoring and hence a likely range is given in Table 1.

For the majority of the applications, there is a still long way to go before full-scale systems are proven in a real-world environment. Apart from the intrinsic complexity of the targeted industrial processes and hostile environmental conditions where the electrostatic sensors to be installed, oversimplified assumptions about the nature of measurement problems and practical conditions are the main reasons for the underdevelopment.

A number of key factors have to be considered for a given industrial application of electrostatic sensors. These should include electrode design, signal conditioning electronics, and signal processing algorithms. Other factors such as practical operation, data interpretation, resolution, cost-effectiveness and applicability of an electrostatic sensing or measurement system should also be considered.

Table 1. Summary of applications of electrostatic sensors

Application	Electrodes used	Signal processing methods used	Key variables determined	Technology Readiness Level (Note 1)
Flow measurement of pneumatically conveyed solids [1], [20]–[27]	Rings; Arcs; Rods	RMS; Cross-correlation; filtering	Particle velocity; Relative concentration of solids; Mass flow rate of solids	TRL9 for particle velocity measurement; TRL7 for mass concentration measurement
Measurement of particulate emissions [31]–[34]	Rods	RMS; Cross-correlation; Filtering	Particle mass density; Particle velocity; Mass emission	TRL9 for particle mass density measurement;

				TRL6 for particle velocity and mass emission measurement
Monitoring of fluidised beds [39]–[50]	Arcs; Wire mesh; Probes	RMS; Cross-correlation; Hilbert-Huang transform; Wavelet transform; Soft computing	Particle velocity; Relative concentration of solids; Charge distribution; Moisture content of solids	TRL4
On-line particle sizing [54], [56]–[58]	Wire mesh; Rings	RMS Signal power ratio Frequency analysis	Mean particle size	TRL1
Burner flame monitoring [66]–[71]	Wires; Probes; Strips	RMS; Cross-correlation; Frequency analysis	Ion density; Flame boundary; Flame speed; Oscillation frequency	TRL2
Speed and radial vibration measurement of mechanical systems [73]–[78], [84]–[86]	Strips	Autocorrelation; Cross-correlation; Frequency analysis; Hilbert-Huang transform	Linear speed; Rotational speed; Vibration frequency; Vibration displacement	TRL4
Condition monitoring of power transmission belts [10], [89]–[91]	Strips	Cross-correlation; Frequency analysis	Axial velocity; Transverse vibration; Operating deflection shape	TRL3
Condition monitoring of mechanical wear [93]–[116]	Rings; Buttons	RMS; Frequency analysis; Independent component analysis; Shaft order analysis; Soft computing	Activity level; Event rate; Energy distribution	TRL3-TRL4
Human activity monitoring [117]–[135]	Disks; Plates; Strips; Wire	Frequency analysis; Localisation; Soft computing;	Respiration rate; Hand gesture and position; Walking gate; Indoor location	TRL3-TRL4

Note 1:
TRL1 – Basic principles observed
TRL2 – Technology concept formulated
TRL3 – Experimental proof of concept
TRL4 – Technology validated in lab
TRL5 – Technology validated in relevant environment (industrially relevant environment in the case of key enabling technologies)
TRL6 – Technology demonstrated in relevant environment (industrially relevant environment in the case of key enabling technologies)
TRL7 – System prototype demonstration in operational environment
TRL8 – System complete and qualified
TRL9 – Actual system proven in operational environment (competitive manufacturing in the case of key enabling technologies; or in space)

B. Electrode Design and Sensor Arrays

Electrodes of a diverse range of shapes have been used in pervious and existing applications of electrostatic sensors. Ring and arc type electrodes are preferred in most flow metering applications as they are physically non-restrictive to the fluid flow in the duct or fluidised bed and hence do not suffer

from wear problems. Strip electrodes are the simplest for the measurement and monitoring of mechanical systems and processes as they are produced as part of the printed circuit board (Fig. 27). For a given application, the electrode design should be optimised in terms of physical dimensions, geometrical shape, manufacturing, installation and maintenance. Meanwhile, the fundamental characteristics of electrostatic sensors, including spatial sensitivity, spatial filtering effect, sensing volume and sensing field uniformity, will need to be considered. Both analytical modelling and finite element modelling have been utilised to optimise the design and geometry of the electrodes. This trend is expected to continue over the years to come and electrodes with some more complex shapes will emerge to achieve optimised sensor properties and enhanced dynamic performance of the sensing system. However, this entails innovative sensor design and construction as well as the development of novel signal processing algorithms. There have been attempts to improve the sensing field uniformity of a strip-type electrostatic sensor through a differential arrangement of two electrodes with different axial widths [137].

To enhance the overall sensitivity of an electrostatic sensor, a preamplifier will be built together with the electrode whilst a secondary amplifier will be used to control the overall gain and frequency bandwidth of the sensing system. The hostile environment where the electrostatic sensors will be installed will be considered so that the sensors are able to withstand high temperature, high moisture content, abrasion of fast moving particle and mechanical vibration.

It is clear that electrostatic sensor arrays with three or more electrodes in conjunction with simple data fusion algorithm have been successfully deployed in a number of applications [27], [71],[74], [91] to achieve enhanced performance of a measurement system in terms of repeatability, rangeability, accuracy, response time and robustness as well as spatial coverage. It is likely that this trend of using one dimensional linear arrays will continue over the next few years. Meanwhile, two dimensional electrostatic linear sensor arrays with a reasonably good spatial resolution will emerge to visualise an area of interest in the presence of electrostatic charge [138]. This imaging concept with a two dimensional electrostatic sensor array and associated electronics is comparable to CCD (charge coupled devices) based optical imaging. However, the target to be visualised has to be close enough to the sensor array due to the inherent limitation of the spatial resolution of electrostatic sensors [138].

Over the past ten years there have been some attempts to develop a technique, which is referred to as ElectroStatic Tomography (EST). The idea is to use an array of electrostatic sensors on the circumference of a circular pipe together with a reconstruction algorithm to obtain the cross-sectional distributions or images of solids in the pipe [139]–[143]. EST is comparable to other electrical tomographic methodologies such as ECT in terms of sensor arrangement, image reconstruction and spatial resolution. However, the fundamental principle of EST is flawed as electrostatic charge appears only on the surface of solids and hence reliable reconstruction of flow patterns or images is impossible. For this very reason, details of EST are excluded in this review.

It is likely that electrostatic sensors will be combined with other sensors such as those operating on acoustic/ultrasonic, capacitive, optical or electromagnetic principles to resolve some of the measurement and monitoring challenges or to enhance the performance of an existing measurement technique. Such a strategy is to make the best use of each sensing principle in order to achieve the functionality and operability of an integrated system, which is otherwise impossible to realise with any of the sensors on their own. For instance, there have already been attempts to combine electrostatic sensors with Acoustic Emission (AE) sensors for the mass flow measurement of pneumatically conveyed particles [144], as shown in Fig. 42, and for the monitoring of mechanical wear [111]. Electrostatic and capacitive sensors have also been integrated to measure the volumetric concentration of biomass-coal-air three-phase flow in a duct [145].

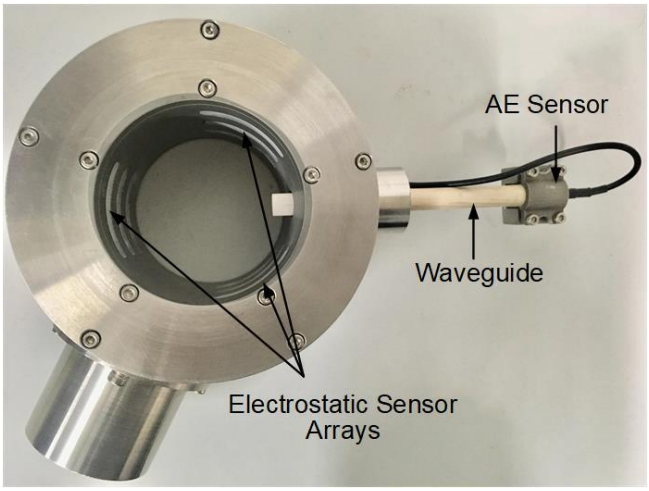

Fig. 42. Integrated electrostatic and AE sensors for mass flow measurement of pneumatically conveyed particles [144].

C. Signal Conditioning Electronics

In most applications that have been reviewed, the induced charge or potential on the electrode is very weak, which poses high demand on the signal conditioning electronics. It has been one of the core research topics in recent years to develop signal conditioning units with high sensitivity, high accuracy, better stability and low noise. Common techniques for measurement of low-level current and voltage discussed comprehensively in Ref. [8] can be used to enhance the circuit performance. Notably, significant research effort has been devoted to enhance the circuit for electric potential measurement, as shown in Fig. 6, because of the low amplitude of the source potential, the high source impedance due to low signal frequency, the very small coupling capacitance between the electrode and the measured object, as well as the high-level electromagnetic interference. Fig. 43 illustrates typical electronic techniques for the acquisition of high-quality electric potential signals [11], [119], [146]. The unavailability of a high-value bias resistor (in the order of TΩ) is alleviated using the bootstrapping technique that exploits positive feedback to boost the effective input impedance at the expense of noise and stability. The stray capacitance C_x is reduced by surrounding the input terminal with a low-impedance guard driven to the same potential as the input by a unity-gain amplifier. The leakage current that degrades the input impedance and the electromagnetic interference is also minimised by the active guard. Meanwhile, the input capacitance of the amplifier can be compensated for by a neutralisation circuit, which provides a positive feedback by injecting part of the output to the input through a capacitor. When the input capacitance is completely negated by adjusting the feedback strength, the gain of the analogue front end is virtually invariant with respect to the coupling capacitance C_S [146], which is analogous to homogenisation of the spatial sensitivity of the sensor.

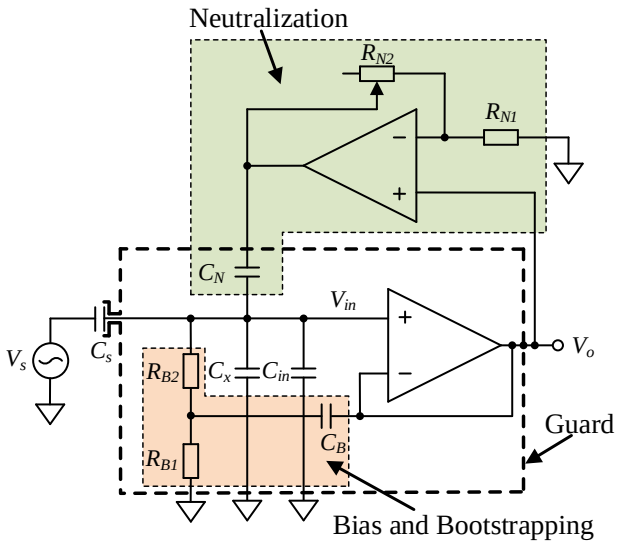

Fig. 43. Typical techniques for electric potential measurement.

The electrode and the signal conditioning circuit can be integrated to realise a self-contained sensor module. The EPIC sensor developed by Prance *et al*. [123], [124] has been commercialised and supplied in a compact custom package with a few connecting leads. The modularisation greatly simplifies the design of the sensing system, enhances its reliability and expands the application area of this technique. Instead of using discrete off-the-shelf amplifiers, an integrated circuits (IC) approach has been adopted by Chi *et al.* [147] to enable enhanced circuit characteristics and higher signal quality.

There has been a surge of research on MEMS electric field sensors in recent years [7]. Although such sensors are mainly designed to measure the strength of static electric field, they are also applicable to varying electric field if the modulation frequency is removed from the signal. Miniaturisation of the sensor opens possibility for array sensing and imaging of the electric field.

In the era of Industry 4.0, smart sensors are the cornerstone of building IoT (Internet of Things) networks and smart factories. It is likely that electrostatic sensors may be integrated with other electronic features such as analogue-to-digital conversion, digital signal processing and wireless communication capabilities [10]. A smart electrostatic sensor can not only measure the parameters of a physical system or process, but also implement other high-level functionalities such as self-calibration and adjustment, fault detection and self-diagnosis. Soft-computing algorithms can also be implemented on an embedded microprocessor with the machine learning models pre-trained off-line on a powerful computer, enabling an edge computing paradigm.

D. Signal Processing Methods

Signal processing is an essential step to convert the original signals from electrostatic sensors to meaningful information. A range of methods are available for processing of the signals from electrostatic sensors or sensor arrays. The signals are usually processed in the time domain, frequency domain or time-frequency domain to present the information in terms of quantifiable variables. Meanwhile, signal processing algorithms are deployed to improve the quality of signals from electrostatic sensors through denoising, decomposition or feature extraction. Correlation, power spectral analysis, Hilbert-Huang transform and wavelet transform have all been deployed as useful tools to characterise and enhance the electrostatic sensor signals. Different processing methods resolve the signal series from different aspects of the application. For example, the RMS magnitude of a sensor signal indicates the overall variability of a target system or process being monitored.

The correlation signal processing algorithm has played a very important part in the use of two electrostatic sensors for the velocity measurement of moving targets. However, the signals from electrostatic sensors are usually contaminated by different types of noise in practical applications, particularly strong common-mode noise due to power supply interference and mechanical vibration. An improved correlation algorithm (R_{mod}) has been proposed to suppress the common-mode noise [81], which is defined as

$$R_{\mathrm{mod}} = R_{s_1 s_1} + R_{s_2 s_2} - R_{s_1 s_2} - R_{s_2 s_1} \tag{20}$$

where R_{s1s1} and R_{s2s2} are the autocorrelations of the two contaminated signals, S_1 and S_2, respectively and R_{s1s2} and R_{s2s1} are the mutual correlation correlations of the two signals. This algorithm has been deployed successfully in the measurement of rotational speed with improved accuracy, rangeability, repeatability and robustness [81]. It is likely that this improved correlation algorithm, either alone or in conjunction with other algorithms, will be utilised in other application areas of electrostatic sensors to achieve enhanced performance and operability of the measurement systems, especially in harsh or extreme environmental conditions.

Hilbert-Huang transform, as a time-frequency domain method, usually outperforms the conventional Fourier transform and wavelet transform to deal with nonlinear and nonstationary signals. Two ring-shaped electrostatic sensors with an axial width of 2 mm and 10 mm, respectively, have been employed to measure gas-solid two-phase flow [149]. Hilbert-Huang transform was utilised to extract the features from the signals to characterise the change in solids concentration [149]. Through empirical mode decomposition, the discrete time domain signal $x(n)$ can be represented in terms of a linear function:

$$x(n) = \sum_{i=1}^{N} c_i(n) + r(n) \tag{21}$$

where n=1, 2,…, L, $c_i(n)$ corresponds to the intrinsic mode functions (IMFs), $r(n)$ the residue of the signal, N the number of IMFs and L the data length.

By applying Hilbert transform to each IMF, a complex representation of IMF $d_i(n)$ is obtained:

$$d_i(n) = c_i(n) * \frac{1}{\pi n} \tag{22}$$

where * represents convolution.

Through the analysis of IMFs of the electrostatic sensor signals, it was found that IMF2 contains most of the energy in the signal from the 2-mm wide sensor while the energy of IMF3 has the highest energy fraction in the signal from the 10-mm wide sensor.

Hilbert-Huang transform has also been used to analyse the signals from a pair of strip-shaped electrostatic sensors to detect the radial vibration of a rotating shaft over the speed range between 400 rpm and 600 rpm [85]. Through Hilbert-Huang transform a total of 9 IMFs with different frequency ranges were obtained from each sensor signal. Results have demonstrated that the eccentric shaft raises the rotating frequency and introduces harmonic frequency components.

Sun *et al.* [43] applied electrostatic sensor arrays to characterise the particle flow in the riser of a CFB. Several signal processing methods, including Hilbert-Huang transform, V-statistic analysis and wavelet transform were combined to characterise the clusters near the wall in the riser. Distinct characteristics of the signals were observed in the Hilbert spectra of the signals. The energy distributions of the IMFs were broadened and shift towards the lower frequency band with the solid flux due to the

enhanced cluster formation and motion, but were narrowed and shift towards the higher frequency band with the superficial gas velocity.

An adaptive decomposition method based on discrete wavelet transform is proposed by Wang *et al* [150] to separate the signal component due to charge induction and that due to direct charge transfer on a circular electrostatic sensor for gas-solid flow measurement. The sensor signal was decomposed into seven components. Results have shown that the first three components are mostly noise whereas the later three components yield higher correlation coefficients and hence can be used to reconstruct the signal element due to the induced charge. Zhang *et al*. [29] proposed to improve the sensing field uniformity of a circular electrostatic sensor by decomposing the power spectrum of the sensor output.

With the increasing use of electrostatic sensor arrays and smart sensors in a variety of applications, a high number of signals are to be processed. To extract useful features from such sensing systems, more advanced signal processing and data fusion techniques are expected to emerge in the near future.

E. Soft Computing and Machine Learning

Principal soft computing techniques include machine learning, evolutionary computation, fuzzy logic and probabilistic reasoning. These techniques have the ability of handling highly complex, non-linear and dynamic problems which are impossible to complete through analytical methods. There have been significant recent developments in deploying soft computing and machine learning algorithms in conjunction with sensors to tackle flow metering challenges [151]. For instance, a combination of electrostatic sensors and soft computing algorithms have been attempted for gas-solid two-phase or three-phase flow measurement and measurement of moisture contents in solids [50]. Yan *et al*. [152] applied a single ring-shaped electrostatic sensor and backpropagation artificial neural networks (BP-ANNs) to measure the velocity and mass flowrate of pneumatically conveyed solids. A total of nine features were extracted from the sensor signal in the time and frequency domains. The input features to the BP-ANN models were selected through Principal Component Analysis (PCA) to minimise the corrected input data. Two three-layer BA-ANN models were developed to estimate the solid velocity and mass flowrate, respectively. Experimental work was conducted with salt particles on a 50 mm bore test rig with expected

velocity from 10 to 30 m/s. Results demonstrated that the relative errors of both particle velocity and mass flowrate measurements were mostly within ±15%. Wang *et al*. [153] integrated a ring-shaped electrostatic sensor and a capacitive sensor with eight electrodes to measure biomass-coal-air three-phase flow. An Adaptive Network based Fuzzy Inference System (ANFIS) was developed to measure solid phase concentrations. The ANFIS model takes the RMS values of electrostatic sensor signals and mean values of the capacitive sensor signals as input features and gives outputs of biomass concentration and pulverised coal concentration, respectively. Experimental tests were conducted on a 36 mm bore horizontal quartz glass pipe with the volumetric concentrations of 0.0079% to 0.04354% for pulverised coal and 0.01129% to 0.06330% for sawdust. Experimental results have shown that the relative errors of biomass and pulverised coal flows were within 2.0% and 0.7%, respectively. In order to reduce the effect of flow regimes on the measurement of solids concentrations, an Extreme Learning Machine (ELM) model was developed for flow regime identification, based on the sub-band energies of electrostatic sensor signals [154]. Adaptive Wavelet Neural Network (AWNN) models taking the RMS values of electrostatic sensor signals and mean values of the capacitive sensor signals were established to estimate biomass and coal concentrations for a specific flow regime. Experimental tests were conducted on a 94 mm bore horizontal pipe, covering stratified, annual and core flow regimes. The method yielded a maximum relative error of 1.7% for biomass and 1.2% for pulverised coal. However, the time taken for the training, identification and prediction processes was significantly reduced with reference to the ANFIS method.

To measure the mass flowrate of particles in a pneumatic conveying pipe, Abbas *et al.* [155] proposed a multi-modal sensing platform along with machine learning models. The sensing platform consists of an array of electrostatic sensors and temperature, humidity and differential-pressure transducers. A variable selection algorithm based on partial mutual information was used to select important features from the signals in the time and frequency domains. Machine learning models, including ANN, Support Vector Machine (SVM) and Convolution Neural Network (CNN) were established and evaluated, respectively, to estimate the mass flowrate of particles. Experimental data was collected on a test rig under the air velocity of 18 m/s and mass flowrate of solid particles ranging from

3.2 g/s to 56.8 g/s. Results have shown that the SVM model outperforms ANN and CNN with a relative error less than ±10%.

There is a clear trend that soft computing algorithms are being combined with electrostatic sensors and sensor arrays to tackle some measurement challenges or enhance the performance of existing measurement or monitoring systems. With advances of soft computing techniques in dealing with uncertain, ambiguous, imprecise, incomplete and subjective data, soft computing models are expected to play a more and more important part in the electrostatic sensing and measurement systems.

F. Further Development of Current Applications and Possible New Applications

Research on applications of electrostatic sensors are progressing rapidly. Some further developments are being made to the applications, as discussed in Section III. There has been attempts to achieve continuous monitoring of the number of particulates in the range between 2.02×10^{11} and 1.03×10^{12} particles/m^3 with particle size ranging from 50 nm to several microns [156]. The aerosol particles were actively charged using a corona diffusion and field charger. However, the key sensing and conditioning element was a Faraday Cup. Further work on the use of a corona charger with a passive electrostatic sensor instead of a Faraday Cup should be conducted. Wire-mesh and ring shaped electrostatic sensors have been attempted for on-line continuous sizing of particles in a pipe. However, significant further research is required in this direction, including the use of electrodes in different shapes and dimensions and the development of effective signal processing algorithms. Electrostatic sensors have also been used to investigate the electrification of wind-blown sand to prevent damage to air traffic [158]. Significant research has been undertaken on the use of active ion current probes for flame detection or monitoring where the electrodes are biased using an external voltage source [69], [70], [159]–[162]. However, limited research has been conducted to utilise passive electrostatic sensors to monitor the flame characteristics [71], [72]. Further development is required to assess the efficacy of electrostatic sensors for advanced flame monitoring in comparison with the ion current detection methods. The technique of human activity monitoring has been applied to monitor animal physiology and behaviors. González-Sánchez *et al*. [163] and Noble *et al*. [164] monitored the respiration, heart rate and various motor behaviors of mice using the

EPIC sensor in laboratory environments. It is expected that the electrostatic sensing technique will be explored for the tracking and detection of animals in very different settings.

In addition to further developments of current applications, new applications are likely to emerge over the next few years. A self-powered proximity sensor through electrostatic induction has been developed with potential applications in touchpads, robotics and safety-monitoring devices [165]. In the military field, an array of electrostatic field sensor has been used for the detection of a charged bullet [166]. In the agricultural sector, electrostatic sensors are used to measure the size of sprayed droplets [167]. Given the fact that electrostatic charge is ubiquitous in the world, applications of electrostatic sensors will continue to expand, thus providing a relatively simple but effective method of process monitoring in a vast spectrum of fields.

To enable a wider applicability of the electrostatic sensing technique where the target to be monitored is metallic, small electret markers may be placed on the surface of the target. This strategy has been successfully deployed in the rotational speed measurement and vibration monitoring of a metallic shaft [86]. Electrets are dielectric materials that are in a quasi-permanent electric polarisation state (electric charges or dipole polarisation). They are electrostatic dipoles, equivalent to permanent magnets but in electrostatics, which are able to maintain electrostatic charges on their surface through time and can keep an electric field for years due to the charge trapping phenomenon [168]. Electret films allow the electrostatic sensors to be applied to monitor and measure of systems and processes involving metallic objects. Significant further research is required to optimise the number and geometric design of electret markers for a given application and to assess the suitability of electret markers to work with electrostatic sensors for a wide range of applications.

V. CONCLUSIONS

This review has attempted to appraise all electrostatic sensors for all known applications and identify the state-of-the-art in developing them further and related signal conditioning and processing techniques. Possible trends in future development are also predicted. The authors are aware that there are publications and inventions which are not included in this review for various reasons.

Electrostatic sensors have notable advantages over other sensor types in terms of simplicity in electrode design and installation, high sensitivity, fast response, wide accessibility and good robustness. In view of these advantages, electrostatic sensors and sensor arrays should be preferentially considered for applications where there is a source of electrostatic charge. This review of the state-of-the-art in electrostatic sensors and their applications has indicated that excellent progress has been made in the development and deployment of electrostatic sensors for the flow measurement of pneumatically conveyed solids and for the measurement of particulate emissions over the past ten years. However, there is still a long way to go before we can see fully operational systems in other industrial sectors. It is believed that substantial development work is required to advance the electrostatic sensing techniques for many real world applications with currently low technology readiness levels. This is particularly true for the monitoring of fluidised beds, on-line particle sizing, burner flames, mechanical wear and vibration, and human activities. The electrostatic imaging with a two dimensional linear sensor array is an encouraging concept. Further development of this emerging technique in the next few years is expected.

With the continuous advances in sensor materials, electronic components and signal processing algorithms, it is becoming increasingly feasible to develop smart electrostatic sensors and sensor arrays, enabling multiple-channel measurement and integrated monitoring functionalities. Correspondingly, different digital signal processing algorithms should be applied in parallel to analyse the signals stemming from different electrostatic charging behaviours of systems, processes and human activities. It will be interesting to read further developments and new applications of electrostatic sensors for the measurement and monitoring of industrial systems and processes or human activities in the next decade.

ACKNOWLEDGMENT

This work was supported by the National Natural Science Foundation of China under Grant 61673170, Grant 61603135 and Grant 51827808 and Engineering and Physical Sciences Research Council of the UK under Grant EP/F061307/1.

REFERENCES

[1] Y. Yan, B. Byrne, S. Woodhead and J. Coulthard, Velocity measurement of pneumatically conveyed solids using electrodynamic sensors, Meas. Sci. Technol. 6 (1995) 515–537.

[2] L. Peng, Y. Zhang and Y. Yan, Characterization of electrostatic sensors for flow measurement of particulate solids in square-shaped pneumatic conveying pipelines, Sens. Actuator A-Phys. 141 (2008) 59–67.

[3] S. Zhang, Y. Yan, X. Qian and Y. Hu, Mathematical modelling and experimental evaluation of electrostatic sensor arrays for the flow measurement of fine particles in a square-shaped pipe, IEEE Sens. J. 16 (2016) 8531–8541.

[4] S. Zhang, S. Wu, X. Qian and Y. Yan, Profiling of pulverized fuel flow in a square-shaped pneumatic conveying pipe using electrostatic sensor arrays, in IMEKO, Belfast, UK, 3–6 September, 2018.

[5] X. Qian and Y. Yan, Flow Measurement of biomass and blended biomass fuels in pneumatic conveying pipelines using electrostatic sensor-arrays, IEEE Trans. Instrum. Meas. 61 (2012) 1343–1352.

[6] Y. Cui, H. Yuan, X. Song, L. Zhao, Y. Liu and L. Lin, Model, design and testing of field mill sensors for measuring electric fields under high-voltage direct-current power lines, IEEE Trans. Ind. Electron. 65 (2018) 608–615.

[7] Y. Zhu, Micro and Nano Machined Electrometers, Singapore, Springer, 2020.

[8] Low Level Measurements Handbook: Precision DC Current, Voltage, and Resistance Measurements, 7th ed., Keithley Instruments Inc., 2016.

[9] Y. Hu, Y. Yan, X. Qian and W. Zhang, A comparative study of induced and transferred charges for mass flow rate measurement of pneumatically conveyed particles, Powder Technol. 356 (2019) 715–725.

[10] Y. Hu, S. Zhang, Y. Yan, L. Wang, X. Qian and L. Yang, A smart electrostatic sensor for online condition monitoring of power transmission belts, IEEE Trans. Ind. Electron. 64 (2017) 7313–7322.

[11] E. Spinelli and M. Haberman, Insulating electrodes: a review on biopotential front ends for dielectric skin-electrode interfaces, Physiol. Meas. 31 (2010) 183–198.

[12] H. Prance, P. Watson, R. J. Prance and S. T. Beardsmore-Rust, Position and movement sensing at metre standoff distances using ambient electric field, Meas. Sci. Technol. 23 (2012) 115101.

[13] L. Wang, Y. Yan, Y. Hu and X. Qian, Rotational speed measurement using single and dual electrostatic sensors, IEEE Sens. J. 3 (2015) 1784–1793.

[14] Y. Yan, Guide to the flow measurement of particulate solids in pipelines, Part 1: fundamentals and principles, Powder Handling Proc. 13 (2001) 343–352.

[15] Y. Zheng and Q. Liu, Review of techniques for the mass flow rate measurement of pneumatically conveyed solids, Measurement 44 (2011) 589–604.

[16] S. Matsusaka, H. Maruyama, T. Matsuyama and M. Ghadiri, Triboelectric charging of powders: a review, Chem. Eng. Sci. 65 (2010) 5781–5807.

[17] J. B. Gajewski, Electrostatic nonintrusive method for measuring the electric charge, mass flow rate, and velocity of particulates in the two-phase gas–solid pipe flows- Its only or as many as 50 years of historical evolution, IEEE Trans. Indus. Appl. 44 (2008) 1418–1430.

[18] J. Li, F. Fu, A. Li, C. Xu and S. Wang, Velocity characterization of dense phase pneumatically conveyed solid particles in horizontal pipeline through an integrated electrostatic sensor, Int. J. Multiphase Flow 76 (2015) 198–211.

[19] J. Shao, J. Krabicka and Y. Yan, Velocity measurement of pneumatically conveyed particles using intrusive electrostatic sensors, IEEE Trans. Instrum. Meas. 59 (2010) 1477–1484.

[20] X. Qian, Y. Yan, J. Shao, L. Wang, H. Zhou and C. Wang, Quantitative characterization of pulverised coal and biomass-coal blends in pneumatic conveying pipelines using electrostatic sensor arrays and data fusion techniques, Meas. Sci. Technol. 23 (2012) 085307.

[21] C. Xu, J. Li, and S. Wang. A spatial filtering velocimeter for solid particle velocity measurement based on linear electrostatic sensor array, Flow Meas. Instrum. 26 (2012) 68–78.

[22] W. Zhang, C. Wang, Y. Wang. Parameter selection in cross-correlation-based velocimetry using circular electrostatic sensors, IEEE Trans. Instrum. Meas., 59 (2010) 1268–1275.

[23] J. R. Coombes, Y. Yan, Measurement of velocity and concentration profiles of pneumatically conveyed particles using an electrostatic sensing array, IEEE Trans. Instrum. Meas. 65 (2016) 1139–1148.

[24] C. Xu, S. Wang, G. Tang, D. Yang and B. Zhou, Sensing characteristics of electrostatic inductive sensor for flow parameters measurement of pneumatically conveyed particles, J. Electrostat. 65 (2007) 582–592.

[25] C. Wang, J. Zhang, W. Zheng, W. Gao and L. Jia, Signal decoupling and analysis from inner flush-mounted electrostatic sensor for detecting pneumatic conveying particles, Powder Technol., 305 (2017) 197–205.

[26] X. Qian, D. Shi, Y. Yan, W. Zhang and G. Li, Effects of moisture content on electrostatic sensing based mass flow measurement of pneumatically conveyed particles, Powder Technol. 311 (2017) 579–588.

[27] X. Qian, Y. Yan, X. Huang and Y. Hu, Measurement of the mass flow and velocity distributions of pulverised fuel in primary air pipes using electrostatic sensing techniques, IEEE Trans. Instrum. Meas. 66 (2017) 944–952.

[28] X. Qian, X. Huang, Y. Hu and Y. Yan, Pulverised coal flow metering on a full-scale power plant using electrostatic sensor arrays, Flow Meas. Instrum., 40 (2014) 185–191.

[29] J. Zhang, R. Cheng, B. Yan and M. Abdalla, Improvement of spatial sensitivity of an electrostatic sensor for particle flow measurement, Flow Meas. Instrum. 72 (2020) 101713.

[30] X. Qian, J. Zhao and X. Huang, Investigations into the blockage of pulverised fuel pipes on coal-fired boilers using an electrostatic sensor system, Powder Technol. in press.

[31] Y. Yan, Continuous measurement of particulate emissions, IEEE Instrum. Meas. Mag. 8 (2005) 35–39.

[32] W. Averdieck, Continuous particulate monitoring, in Environmental, Instrumentation and Analysis Handbook, Chapter 15, John Wiley, 2005.

[33] ENVEA UK Ltd. Guide to application parameters for technologies, http://www.pcme.com, 2020 (accessed on 2 September 2020).

[34] Y, Yan and J. Ma, Measurement of particulate velocity under stack flow conditions, Meas. Sci. Technol. 11 (2000) 59–65.

[35] J. Sun and Y. Yan, Non-intrusive measurement and hydrodynamics characterization of gas–solid fluidised beds: a review, Meas. Sci. Technol. 27 (2016) 112001.

[36] F. Fotovat, X. Bi and J. Grace, Electrostatics in gas-solid fluidised beds: A review, Chem. Eng. Sci., 173 (2017) 303–334.

[37] P. Mehrani, M. Murtomaa and D. Lacks, An overview of advances in understanding electrostatic charge buildup in gas-solid fluidised beds, J. Electrostat. 87 (2017) 64–78.

[38] F. Fotovat, X. Bi, and J. Grace, A perspective on electrostatics in gas-solid fluidised beds: Challenges and future research needs, Powder. Technol. 329 (2018) 65–75.

[39] W. Zhang, Y. Cheng, C. Wang, W. Yang and C. Wang, Investigation on hydrodynamics of triple-bed combined circulating fluidised bed using electrostatic sensor and electrical capacitance tomography, Ind. Eng. Chem. Res. 52 (2013) 11198–11207.

[40] W. Zhang, Y. Yan, Y. Yang and J. Wang, Measurement of flow characteristics in a bubbling fluidised bed using electrostatic sensor arrays, IEEE Trans. Instrum. Meas. 65 (2016) 703–712.

[41] Y. Yao, Q. Zhang, C. Zi, Z. Huang, W. Zhang, Z. Liao, J. Wang, Y. Yang, Y. Yan and G. Han, Monitoring of particle motions in gas-solid fluidised beds by electrostatic sensors, Powder. Technol. 308 (2017) 461–471.

[42] J. Sun and Y. Yan, Characterization of flow intermittency and coherent structures in a gas–solid circulating fluidised bed through electrostatic sensing, Ind. Eng. Chem. Res., 55 (2016) 12133–12148.

[43] J. Sun and Y. Yan, Non-intrusive characterisation of particle cluster behaviours in a riser through electrostatic and vibration sensing, Chem. Eng. J. 323 (2017) 381–395.

[44] W. Zhang, Y. Yan, X. Qian, Y. Guan and K. Zhang, Measurement of charge distributions in a bubbling fluidised bed using wire-mesh electrostatic sensors, IEEE Trans. Instrum. Meas. 66 (2017) 522–534.

[45] J. Sun, Y. Yang, Q. Zhang, Z. Huang, J. Wang, Z. Liao and Y. Yang, Online measurement of particle charge density in a gas-solid bubbling fluidised bed through electrostatic and pressure sensing, Powder. Technol. 317 (2017) 471–480.

[46] Q. Shi, Q. Zhang, G. Han, W. Zhang, J. Wang, Z. Huang, Y. Yao, Y. Yang, W. Wu and Y. Yan, Simultaneous measurement of electrostatic charge and its effect on particle motions by electrostatic sensors array in gas-solid fluidised beds, Powder. Technol. 312 (2017) 29–37.

[47] C. He, X. Bi, J. Grace, Monitoring electrostatics and hydrodynamics in gas–solid bubbling fluidised beds using novel electrostatic probes, Ind. Eng. Chem. Res. 54 (2015) 8333–8343.

[48] C. He, X. Bi and J. Grace, Simultaneous measurements of particle charge density and bubble properties in gas-solid fluidised beds by dual-tip electrostatic probes, Chem. Eng. Sci., 123 (2015) 11–21.

[49] W. Zhang, X. Cheng, Y. Hu and Y. Yan, Measurement of moisture content in a fluidised bed dryer using an electrostatic sensor array, Powder. Technol. 325 (2018) 49–57.

[50] W. Zhang, X. Cheng, Y. Hu and Y. Yan, Online prediction of biomass moisture content in a fluidised bed dryer using electrostatic sensor arrays and the Random Forest method, Fuel 239 (2019) 437–445.

[51] N. Malumbazo, N. J. Wagner and J. R. Bunt, The impact of particle size and maceral segregation on char formation in a packed bed combustion unit, Fuel 111 (2013) 350–356.

[52] Particle size analysis–Laser diffraction methods, BSI Standards Limited, BS ISO 13320, 2019.

[53] L. Gao, Y. Yan, G. Lu and R.M. Carter, On-line measurement of particle size and shape distributions of pneumatically conveyed particles through multi-wavelength based digital imaging, Flow Meas. Instrum., 27 (2012) 20–28.

[54] J. Zhang and Y. Yan, On-line continuous measurement of particle size using electrostatic sensors, Powder. Technol. 135–136 (2003) 164–168.

[55] W. Chen, J. Zhang, T. Donohue, K. Williams, R. Cheng, M. Jones and B. Zhou, Effect of particle degradation on electrostatic sensor measurements and flow characteristics in dilute pneumatic conveying, Particuology 33 (2017) 73–79.

[56] T. Tajdari, M. Rahmat and N. Wahab, New technique to measure particle size using electrostatic sensor, J. Electrost. 72 (2014) 120–128.

[57] X. Qian, X. Wei, Y. Yan and D. Shi, Particle size estimation of pulverized fuel in pneumatic pipelines using electrostatic sensing techniques, Proceedings of the XXII World Congress of the International Measurement Confederation, Belfast, United Kingdom, 3–7 September, 2018.

[58] F. Abdullah and H. Rahmat, Measurement of particle size using electrostatic sensors, International Conference on Electrical, Control and Computer Engineering, Pahang, Malaysia, 21–22 June, 2011.

[59] A. V. Singh, A. Eshaghi, M. Yu, A. K. Gupta and K. M. Bryden, Simultaneous time-resolved fluctuating temperature and acoustic pressure field measurements in a premixed swirl flame, Appl. Energy, 115 (2014) 116–127.

[60] M. Mazzillo and A. Sciuto, 4H-SiC Schottky photodiodes for ultraviolet flame detection, J. Instrum., 10 (2015) 10029.

[61] D. Sun, G. Lu, H. Zhou, Y. Yan and S. Liu, Quantitative assessment of flame stability through image processing and spectral analysis, IEEE Trans. Instrum. Meas. 64 (2015) 3323–33.

[62] J. Lawton and F. J. Weinburg, Electrical aspects of combustion. Oxford, U. K, Clarendon Press, 1969.

[63] H. F. Calcote, Mechanisms for the formation of ions in flames, Combust. Flame, 1 (1957) 385–403.

[64] M. Balthasa, F. Mauss and H. Wang, A computational study of the thermal ionization of soot particles and its effect on their growth in laminar premixed flames, Combust. Flame 129 (2002) 204–216.

[65] A. B. Fialkov, Investigations on ions in flames, Prog. Energy Combust. Sci. 23 (1997) 399–528.

[66] C. S. Maclatchy and J. W. Forsman, A novel electrostatic probe technique for measuring the ions density in a flame, Combust. Flame 53 (1983) 41–48.

[67] J. Guo, J. M. Goodings, A. N. Hayhurst and S. G. Taylor, A simple method for measuring positive ion concentrations in flames and the calibration of a nebulizer/atomizer, Combust. Flame 133 (2003) 335–43.

[68] L. B. W. Peerlings, Manohar, V. N. Kornilov and P. D. Goey, Flame ion generation rate as a measure of the flame thermo-acoustic response, Combust. Flame 160 (2013) 2490–6.

[69] T. Yokomori, S. Mochida, T. Araake and K. Maruta, Electrostatic probe measurement in an industrial furnace for high-temperature air conditions, Combust. Flame, 150 (2007) 369–79.

[70] F. Li, L. Xu, Z. Cao and M. Du, A chemi-ionization processing approach for characterizing flame flicker behavior, in IEEE Instrumentation and Measurement Technology Conference, 2015, pp. 325.

[71] J. Wu, Y. Hu, Y. Yan, X. Qian and S. Gu, Flicker measurement of burner flames through electrostatic sensing and spectral analysis, in Proceedings of XXII World Congress of the International Measurement Confederation, 2018, pp. 1065: 20022004.

[72] J. Wu, Y. Yan, Y. Hu, L. Shan and W. Xu, Flame boundary measurement using an electrostatic sensor array, in press, IEEE Trans. Instrum. Meas. 2020 (doi:10.1109/TIM.2020.3014753).

[73] Y. Yan, S. J. Rodrigues and Z. Xie, Non-contact strip speed measurement using electrostatic sensing and correlation signal-processing techniques, Meas. Sci. Technol., 22 (2011) 075103.

[74] L. Wang, Y. Yan, Y. Hu and X. Qian, Rotational speed measurement through electrostatic sensing and correlation signal processing, IEEE Trans. Instrum. Meas. 66 (2014) 1190–1199.

[75] L.Wang and Y. Yan, Mathematical modelling and experimental validation of electrostatic sensors for rotational speed measurement, Meas. Sci. Technol. 25 (2014) 115101.

[76] L. Wang, Y. Yan, K. Reda, Comparison of single and double electrostatic sensors for rotational speed measurement, Sensors and Actuators A: Physical 266 (2017) 46–55.

[77] K. Reda, Y. Yan and L. Wang, A comparative study of different shaped electrostatic sensors for rotational speed measurement, in Proceedings of IEEE Sensors Conference, Glasgow, UK, October 30-November 1, 2017.

[78] L. Li, X. Wang, H. Hu and X. Liu, Use of double correlation techniques for the improvement of rotation speed measurement based on electrostatic sensors, Meas. Sci. Technol., 27 (2016) 025004.

[79] L. Lin, H. Hu, Y. Qin and K. Tang, Digital approach to rotational speed measurement using an electrostatic sensor, Sensors, 19 (2019) 2540.

[80] L. Wang, Y. Yan and K. Reda, Enhancing the performance of a rotational speed measurement system through data fusion, in Journal of Physics: Conference Series 1065 - the XXII World Congress of the International Measurement Confederation, Belfast, UK, September 3-6, 2018, pp.072024.

[81] K. Reda and Y. Yan, An improved method for the processing of signals contaminated with strong common-mode periodic noise in correlation velocity measurement, IEEE Sensors Letters 3 (2019), 7001404.

[82] R. B. Randall, State of the art in monitoring rotating machinery - Part 1, Sound Vib. 38 (2004) 14–21.

[83] H. Chaurasiya, Recent trends of measurement and development of vibration sensors, Int. J. Comput. Sci. Iss. 9 (2019) 353–358.

[84] L. Wang, Y. Yan, Y. Hu and X. Qian, Intelligent condition monitoring of rotating machinery through electrostatics sensing and signal analysis, in IEEE International Conference on Smart Instrumentation, Kuala Lumpur, Malaysia, November 26–27, 2013.

[85] L. Wang, Y. Yan, Y. Hu and X. Qian, Radial vibration measurement of rotary shafts through electrostatic sensing and Hilbert-Huang transform, in IEEE International Instrumentation and Measurement Technology Conference, Taipei, Taiwan, May 23–26, 2016, pp.867–871.

[86] K. Reda and Y. Yan, Vibration measurement of an unbalanced metallic shaft using electrostatic sensors, IEEE Trans. Instrum. Meas. 68 (2019) 1467–1476.

[87] P. Catalano, F. Fucci, F. Giametta, G. La Fianza and B. Bianchi, Vibration analysis using a contactless acquisition system, in Proc. SPIE, 2013, pp. 8881:888108.

[88] P. Chiariotti, M. Martarelli and P. Castellini, Exploiting continuous scanning laser Doppler vibrometry in timing belt dynamic characterization, Mech. Syst. Signal Process. 86 (2017) 66–81.

[89] Y. Hu, Y. Yan, L. Wang, X. Qian and X. Wang, Simultaneous measurement of belt speed and vibration through electrostatic sensing and data fusion, IEEE Trans. Instrum. Meas. 65 (2016) 1130–1138.

[90] Y. Hu, Y. Yan, L. Wang and X. Qian, Non-contact vibration monitoring of power transmission belts through electrostatic sensing, IEEE Sens. J. 16 (2016) 3541–3550.

[91] Y. Hu, Y. Yan, L. Yang, L. Wang and X. Qian, Online continuous measurement of the operating deflection shape of power transmission belts through electrostatic charge sensing, IEEE Trans. Instrum. Meas. 66 (2017) 492–501.

[92] Z. Wen, J. Hou and J. Atkin, A review of electrostatic monitoring technology: the state of the art and future research directions, Prog. Aeosp. Sci. 94 (2017) 1–11.

[93] H. Powrie and J. Worsfold, Gas path debris monitoring for heavy-duty gas turbines – a pilot study, in IDGTE Gas Turbine Symposium, 2001, pp. 168–179.

[94] A. Novis and H. Powrie, PHM sensor implementation in the real world – a status report, in IEEE Aerospace Conference, MT, USA, Mar. 4–11, 2006.

[95] H. Powrie and A. Novis, Gas path debris monitoring for F-35 joint strike fighter propulsion system PHM, in IEEE Aerospace Conference, MT, USA, Mar. 4–11, 2006.

[96] Z. Wen, H. Zou and M. G. Pecht, Electrostatic monitoring of gas path debris for aero-engines, IEEE Trans. Reliab. 60 (2011) 33–40.

[97] P. Liu, H. Zou and J. Sun, The electrostatic sensor applied to the online monitoring experiments of combustor carbon deposition fault in aero-engine, IEEE Sens. J. 14 (2014) 686–694.

[98] Y. Fu, H. Zou, R. Wang, P. Liu, J. Cai and Z. Wen, A monitoring experiment for gas path electrostatic probe-type sensor on turbojet Engine, Information Technology Journal 12 (2013) 331-337.

[99] J. Sun, H. Zou, P. Liu and Z. Wen, Experimental study on engine gas-path component fault monitoring using exhaust gas electrostatic signal, Meas. Sci. Technol. 24 (2013) 125107.

[100] Y. Yin, J. Cai, H. Zou, H. Mao, Y. Fu and H. Yan, Experimental investigation on electrostatic monitoring technology for civil turbofan engine, J. Vibroeng. 19 (2017) 967–987.

[101] Z. Wen, X. Ma and H. Zuo, Characteristics analysis and experiment verification of electrostatic sensor for aero-engine exhaust gas monitoring, Measurement 47 (2014) 633–644.

[102] Z. Chen, X. Tang, Z. Hu and Y. Yang, Investigations into sensing characteristics of circular thin-plate electrostatic sensors for gas path monitoring, Chin. J. Aeronaut. 27 (2014) 812–820.

[103] J. Lin, Z. Chen, Z. Hu, Y. Yang and X. Tang, Analytical and numerical investigations into hemisphere-shaped electrostatic sensors, Sensors 14 (2014) 14021–14037.

[104] X. Tang, Z. Chen, Y. Li, Z. Hu and Y. Yang, Theoretical analysis and finite element method simulations on dynamic sensitivity of hemisphere-shaped electrostatic sensors, Adv. Mech. Eng. 8 (2016) 1–16.

[105] T. Addabbo, A. Fort, R. Garbin, M. Mugnaini, S. Rocchi and V. Vignoli, Theoretical characterization of a gas path debris detection monitoring system based on electrostatic sensors and charge amplifiers, Measurement 64 (2015) 138–146.

[106] T. Addabbo, A. Fort, M. Mugnaini, E. Panzardi, S. Rocchi and V. Vignoli, Measurement system based on electrostatic sensors to detect moving charged debris with planar-isotropic accuracy, IEEE Trans. Instrum. Meas. 68 (2019) 837–844.

[107] O.D. Tasbaz, R.J.K. Wood, M. Browne, H.E.G. Powrie and G. Denuault, Electrostatic monitoring of oil lubricated sliding point contacts for early detection of scuffing, Wear 230 (1999) 86–97.

[108] T. J. Harvey, R.J.K. Wood, G. Denuault and H.E.G. Powrie, Effect of oil quality on electrostatic charge generation and transport, J. Electrost. 55 (2002) 1–23.

[109] T. J. Harvey, R.J.K. Wood, G. Denuault and H.E.G. Powrie, Investigation of electrostatic charging mechanisms in oil lubricated tribo-contacts, Tribol. Int. 35 (2002) 605–614.

[110] S. Morris, R.J.K. Wood, T.J. Harvey and H.E.G. Powrie, Electrostatic charge monitoring of unlubricated sliding wear of a bearing steel, Wear 255 (2003) 430–443.

[111] J. Sun, R.J.K. Wood, L. Wang, I. Care and H.E.G Powrie, Wear monitoring of bearing steel using electrostatic and acoustic emission techniques, Wear 259 (2005) 1482–1489.

[112] T.J. Harvey, R.J.K. Wood and H.E.G. Powrie, Electrostatic wear monitoring of rolling element bearings, Wear 263 (2007) 1492–1502.

[113] M. Craig, T.J. Harvey, R.J.K. Wood, K. Masuda, M. Kawabata and H.E.G. Powrie, Advanced condition monitoring of tapered roller bearings, Part1, Tribol. Int., 42 (2009) 1846–1856.

[114] R.C. Liu, H.F. Zou, J.Z. Sun and L. Wang, Simulation of electrostatic oil line sensing and validation using experimental results, Tribol. Int. 105 (2017) 15–26.

[115] H. Mao, H. Zou, H. Wang, Y. Yin and X. Li, Debris recognition methods in the lubrication system with electrostatic sensors, Math. Probl. Eng. (2018) 8043526.

[116] H. Mao, H. Zou and H. Wang, Electrostatic sensor application for on-line monitoring of wind turbine gearboxes, Sensors 18 (2018) 3574.

[117] T. Ficker, Electrification of human body by walking, J. Electrostat. 64 (2006) 10–16.

[118] T. Grosse-Puppendahl, X. Dellangnol, C. Hatzfeld, B. Fu, M. Kupnik, A. Kuijper, M. R. Hastall, J. Scott and M. Gruteser, Platypus – Indoor localization and identification through sensing electric potential changes in human bodies, in 14th Annual International Conference on Mobile Systems, Applications, and Services, Singapore, June 25–30, 2016, pp.17–30.

[119] Y. Sun and X. Yu, Capacitive biopotential measurement for electrophysiological signal acquisition: a review, IEEE Sens. J., 16 (2016) 2832–2853.

[120] H. Prance, P. Watson, R. J. Prance and S. T. Beardsmore-Rust, Position and movement sensing at metre standoff distances using ambient electric field, Meas. Sci. Technol. 23 (2012) 115101.

[121] X. Tang and S. Mandal, Indoor occupancy awareness and localization using passive electric field sensing, IEEE Trans. Instrum. Meas. 68 (2019) 4535–4549.

[122] C. J. Harland, R. J. Prance and H. Prance, Remote monitoring of biodynamic activity using electric potential sensors, in Journal of Physics: Conference Series, 142 (2008) 012042.

[123] R. J. Prance, A. Debray, T. D. Clark, H. Prance, M. Nock, C. J. Harland and A. J. Clippingdale, An ultra-low-noise electrical-potential probe for human-body scanning, Meas. Sci. Technol. 11 (2000) 291–297.

[124] H. Prance, Sensor developments for electrophysiological monitoring in healthcare, Applied Biomedical Engineering 2011, 265–286.

[125] K. Kurita, Detection of human respiration based on measurement of current generated by electrostatic induction, Artif. Life Robot. 15 (2010) 181–184.

[126] Y. Kim and C. Moon, Non-contact gesture recognition using the electric field disturbance for smart device application, Int. J. Multimedia Ubiquit. Eng. 9 (2014) 133–140.

[127] K. Kurita, Noncontact hand motion classification technique for application to human-machine interfaces, IEEE Trans. Ind. Appl. 50 (2014) 2213–2218.

[128] K. Tang, P. Li, C. Wang, Y. Wang and X. Chen, Real-time hand position sensing technology based on human body electrostatics, Sensors 18 (2018) 1677.

[129] K. Takiguchi, T. Wada and S. Toyama, Human body detection that uses electric field by walking, J. Adv. Mech. Des. Syst. Manuf. 1 (2007) 294–305.

[130] M. Li, P. Li, S. Tian, K. Tang and X. Chen, Estimation of temporal gait parameters using a human body electrostatic sensing-based method, Sensors 18 (2018) 1737.

[131] K. Kurita and S. Morinaga, Detection technique of individual characteristic appearing in walking motion, IEEE Access 7 (2019) 139226–139235.

[132] K. Kurita and S. Morinaga, Noncontact detection of movements of standing up from and sitting down on a chair using electrostatic induction, IEEE Sens. J. 19 (2019) 8934–8939.

[133] A. Pouryazdan, D. Roggen, R. J. Prance and H. Prance, Wearable electric potential sensing: a new modality sensing hair touch and restless leg movement, in 2016 ACM International Joint Conference on Pervasive and Ubiquitous Computing, Heidelberg, Germany, Sep. 12-16 2016, pp. 846–850.

[134] G. Cohn, S. Gupta, T. Lee, D. Morris, J. R. Smith, M. S. Reynolds, D. S. Tan and S. N. Patel, An ultra-low-power human body motion sensor using static electric field sensing, in 2012 ACM Conference on Ubiquitous Computing, Pittsburgh, PA, USA, Sep. 5–8, 2012, pp. 99–102.

[135] B. Fu, F. Kirchbuchner, J. v. Wilmsdorff, T. Grosse-Puppendahl, A. Braun and A. Kuijper, Performing indoor localization with electric potential sensing, J. Amb. Intel. Hum. Comp. 10 (2019) 731–746.

[136] H. Mihaly, From NASA to EU: the evolution of the TRL scale in Public Sector Innovation, The Innovation Journal: The Public Sector Innovation Journal, 22 (2017) 1–23.

[137] S. Zhang, Y. Yan, X. Qian, R. Huang and Y. Hu, Homogenization of the spatial sensitivity of electrostatic sensors for the flow measurement of pneumatically conveyed solids in a square-shaped pipe, IEEE Sens. J. 17 (2017) 7516–7525.

[138] B. Qi, W. Zhang, Y. Yan and X. Li, Continuous measurement of charge distribution in a single-jet fluidised bed using an electrostatic sensor array, in IEEE International Instrumentation and Measurement Technology Conference, Dubrovnik, Croatia, May 25–28, 2020.

[139] R.G. Green, M.F. Rahmat, K. Evans, et al., Concentration profiles of dry powders in a gravity conveyor using an electrodynamic tomography system, Meas. Sci. Technol. 8 (1997) 192-197.

[140] M. Machida, B. Scarlett, Process tomography system by electrostatic charge carried by particles, IEEE Sensors J. 5 (2005) 251-259.

[141] B. Zhou, J.Y. Zhang, A novel ECT–EST combined method for gas–solids flow pattern and charge distribution visualization, Meas. Sci. Technol. 24 (2013) 074003.

[142] I.T. Thuku, M.F. Rahmat, Finite-element method modeling in 4 and 16 sensors electric-charge tomography systems for particles moving in pipeline, Flow Meas. Instrum. 38 (2014) 9-20.

[143] H.M. Gao, B.Y. Fan, Y.X. Min, et al., Investigation on the optimized algorithm for electrostatic tomography, Rev. Sci. Instrum. 89 (2018) 085116.

[144] G. Zheng, Y. Yan, Hu Y, W. Zhang, L. Yang and L. Li, Mass flow rate measurement of pneumatically conveyed particles through acoustic emission detection and electrostatic sensing, in IEEE International Instrumentation and Measurement Technology Conference, Dubrovnik, Croatia, May 25–28, 2020.

[145] J. Zhang, H. Hu, J. Dong and Y. Yan, Concentration measurement of biomass/coal/air three-phase flow by integrating electrostatic and capacitive sensors, Flow Meas. Instrum., 24 (2012) 43–49.

[146] Y. M. Chi, S. R. Deiss and G. Cauwenberghs, Non-contact low power EEG/ECG electrode for high density wearable biopotential sensor networks, in 6th International Workshop on Wearable and Implantable Body Sensor Networks, Berkeley, California, USA, June 3–5, 2009.

[147] Y. M. Chi, C. Maier and G. Cauwenberghs, Ultra-high input impedance, low noise integrated amplifier for noncontact biopotential sensing, IEEE. J. Em. Sel. Top. C. 1 (2011) 526–535.

[148] L. Xu, J. Zhang and Y. Yan, A wavelet-based multisensor data fusion algorithm, IEEE Trans. Instrum. Meas. 53 (2004) 1539–1545.

[149] W. Zhang, C. Wang and H. Wang, Hilbert-Huang transform-based electrostatic signal analysis of ring-shape electrodes with different widths, IEEE Trans. Instrum. Meas. 61 (2012) 1209–1217.

[150] C. Wang, N. Zhan, L. Jia, J. Zhang and Y. Li, DWT-based adaptive decomposition method of electrostatic signal for dilute phase gas-solid two-phase flow measuring, Powder Technol., 329 (2018) 199–206.

[151] Y. Yan, L. Wang, T. Wang, X. Wang, Y. Hu and Q. Duan, Application of soft computing techniques to multiphase flow measurement: a review, Flow Meas. Instrum. 60 (2018) 30–43.

[152] Y Yan, L. Xu and Lee P., Mass flow measurement of fine particles in a pneumatic suspension using electrostatic sensing and neural network techniques, IEEE Trans. Instrum. Meas. 55 (2006), 2330–2334.

[153] X. Wang, H. Hu and A. Zhang, Concentration measurement of three-phase flow based on multi-sensor data fusion using adaptive fuzzy interference system, Flow Meas. Instrum. 39 (2014) 1–8.

[154] X. Wang, H. Hu and X. Liu, Multisensor data fusion techniques with ELM for pulverised-fuel flow concentration measurement in cofired power plant, IEEE Trans. Instrum. Meas. 64 (2015) 2769–2780.

[155] F. Abbas, Y. Yan and L. Wang, Mass flow measurement of pneumatically conveyed solids through multi-modal sensing and machine learning, in IEEE International Instrumentation and Measurement Conference, Dubrovnik, Croatia, May 25–28, 2020.

[156] P. Intra, A. Yawootti and N. Tippayawong, An electrostatic sensor for the continuous monitoring of particulate air pollution, Korean J. Chem. Eng. 30 (2013) 2205–2212.

[157] J Zhang and Y Yan, On-line continuous measurement of particle size using electrostatic sensors, Powder Technol. 135-136 (2003) 164–168.

[158] X. J. Zheng, Electrification of wind-blown sand: Recent advances and key issues, Eur. Phys. J. E, 36 (2013) 138.

[159] T. Addabbo, A. Fort, M. Mugnaini, L. Parri, V. Vignoli1, M. Allegorico, M. Ruggiero and S. Cioncolini, Ion sensor-based measurement systems: application to combustion monitoring in gas turbines, IEEE Trans. Instrum. Meas. 69 (2020) 1474–1483.

[160] F. Li, L. Xu, M. Du, L. Yang and Z. Gao, Ion current sensing-based lean blowout detection for a pulse combustor, Combustion and Flame, 176 (2017) 263–271.

[161] A. A.M. Laganá, L. L. Lima, J. F. Justo, B. A. Arruda, M. M.D. Santos, Identification of combustion and detonation in spark ignition engines using ion current signal, Fuel, 227 (2018) 469–477.

[162] Z. Song, X. Zhang, X. Hou, S. Hu, Relationship of the combustion characteristics of natural gas-hydrogen/carbon dioxide mixtures with the ion current and pressure parameters, Journal of the Energy Institute, 92 (2018) 1014–1022.

[163] C. González-Sánchez, J. Fraile, J. Pérez-Turiel, E. Damm, J. G. Schneider, H. Zimmermann, D. Schmitt and F. R. Ihmig, Capacitive sensing for non-invasive breathing and heart monitoring in non-restrained, non-sedated laboratory mice, Sensors 16 (2016) 1052.

[164] D. J. Noble, C. J. MacDowell, M. L. McKinnon, T. I. Neblett, W. N. Goolsby and S. Hochman, Use of electric field sensors for recording respiration, heart rate, and stereotyped motor behaviors in the rodent home cage, J. Neurosci Meth. 277 (2017) 88–100.

[165] J. Zhu, R. Huang and H. Zhu, Proximity sensing of electrostatic induction electret nanoparticles device using separation electrode, AIP Advances 7 (2017) 045016.

[166] M. A. Noras, S. P. Ramsey and B. B. Rhoades, Projectile detection using quasi-electrostatic field sensor array, J. Electrost. 71 (2013) 220–223.

[167] M. Kuna-Broniowski, Electrostatic method to measure the size of the sprayed droplets, in 5th European Workshop on Standardised Procedure for the Inspection of Sprayers, Montpellier, France, Oct. 15–17, 2014.

[168] G. M. Sessler, Physical principles of electrets, in Electrets, New York, USA: Springer-Verlag, 1980.